Journal of Medicinal Chemistry

Article

Synthesis, in vitro, and in cell studies of a new series of [indoline-3,2'-thiazolidine]-based p53 modulators.

Alessia Bertamino, Maria Soprano, Simona Musella, Maria Rosaria Rusciano, Marina Sala, Ermelinda Vernieri, Veronica Di Sarno, Antonio Limatola, Alfonso Carotenuto, Sandro Cosconati, Paolo Grieco, Ettore Novellino, Maddalena Illario, Pietro Campiglia, and Isabel Gomez-Monterrey

J. Med. Chem., **Just Accepted Manuscript** • DOI: 10.1021/jm400311n • Publication Date (Web): 12 Jun 2013

Journal of Medicinal Chemistry is published by the American Chemical Society. 1155 Sixteenth Street N.W., Washington, DC 20036

Synthesis, in vitro, and in cell studies of a new series of [indoline-3,2'-thiazolidine]-based p53 modulators.

Alessia Bertamino,[a] Maria Soprano,[b] Simona Musella,[a] Maria Rosaria Rusciano,[b] Marina Sala,[a] Ermelinda Vernieri,[a] Veronica Di Sarno,[a] Antonio Limatola,[c] Alfonso Carotenuto,[c] Sandro Cosconati,[d] Paolo Grieco,[c] Ettore Novellino,[c] Maddalena Illario,[b] Pietro Campiglia,[a] Isabel Gomez-Monterrey.[c]*

[a]Depart. of Pharmacy, University of Salerno, 84084 Fisciano, Salerno, Italy

[b]Depart. of Cellular and Molecular Biology, University of Naples Federico II, 80131 Naples, Italy

[c]Depart. of Pharmacy, University of Naples Federico II, 80131 Naples, Italy

[d]DiSTABiF, Second University of Naples , 81100 Caserta, Italy

ABSTRACT

Analogs of the previously described spiro[imidazo[1,5-*c*]thiazole-3,3'-indoline]-2',5,7(6H,7aH)-trione p53 modulators, were prepared to explore new structural requirements at the thiazolidine domain for the antiproliferative activity and p53 modulation. In cell, anti-proliferative activity was evaluated against two human tumor cell lines. Derivative 5-bromo-3'-(cyclohexane carbonyl)-1-methyl-2-oxospiro[indoline-3,2'-thiazolidine] (**4n**) emerged as the most potent compound of this series, inhibiting in vitro a 30% of p53-MDM2 interaction at 5μM and the cell growth of different human tumor cells at nanomolar concentrations. Docking studies confirmed the interactions of **4n** with the well known Trp23 and Phe19 clefts explaining the reasons for its binding affinity for MDM2. **4n** at 50 nM is capable to induce the accumulation of p53 protein, inducing significant apoptotic cell death without affecting the cell cycle progression. Comparative studies using nutlin in the same cellular system confirms the potential of **4n** as a tool for increasing understanding of the process involved in the non-transcriptional pro-apoptotic activities of p53.

INTRODUCTION

p53 is the tumor suppressor protein which has been the most intensively studied for nearly 30 years.[1] p53 functions mainly as a transcription factor by binding to specific DNA sequences and by transactivating or repressing a large group of target genes.[2] Through these downstream targets, p53 pathway coordinates cell cycle arrest, DNA repair, apoptosis and senescence to preserve genomic stability and prevent tumor formation in response to cellular insults, including DNA damage, hypoxia, and a deficiency of growth factors or nutrients.[1-4] Recently, novel functions of p53 in metabolism regulation and tumor motility, invasion and metastasis have

been unveiled.[5,6] p53 levels are tightly controlled in unstressed mammalian cells through a continuous cycle of ubiquitylation and degradation by the 26S proteasome, regulated primarily through the interaction of p53 with the ring-finger ubiquitin E3 ligase MDM2.[7] This protein controls the p53 levels through a direct binding interaction that neutralizes p53 transactivation activity, exports nuclear p53, and targets it for degradation via the ubiquitylation-proteasomal pathway.[8-10] Loss of p53 activity, either by deletion, mutation, or MDM2 overexpression, is the most common event in the development and progression of cancer,[11,12] while the restoration of endogenous p53 function results in tumor regression in vivo.[1,13] In this context, the rescue of the impaired p53 activity and re-sensitization to apoptosis in cancer cells by disrupting the MDM2-p53 interaction offers an opportunity for anticancer therapeutics.[14] The tractability of the MDM2-p53 interaction as a drug target has been demonstrated and a number of classes of potent small molecule inhibitors have been developed.[15] Vassilev et al.[16] identified the first group of molecules that target the MDM2-p53 interaction (Figure 1). These imidazoline derivatives, designated Nutlins, specifically bind and dissociate MDM2 from p53, leading to extensive p53 activation and induction of a full-blown p53 response, which can trigger tumour shrinkage in experimental animals. The derivative Nutlin-3 is currently undergoing Phase I clinical evaluation against advanced solid tumors and hematological malignancies. The benzodiazepines[17] and the spiro-oxindole–based compounds[18] are other classes of small molecules that have been found to target the p53-MDM2 interaction. These results led to the preclinical development of TDP665759 and MI-319, which disrupt the binding of MDM2 to p53 in vitro and suppress the growth of tumor cells both in vitro and in vivo. Both compounds limit tumor growth without causing major toxicity in the surrounding tissue. Although these products induce high levels of

p53, these are not sufficient to activate the apoptotic cascade. Other small-molecule inhibitors include chromenotriazolo pyrimidines (1),[19] and oxoindoles (2).[20]

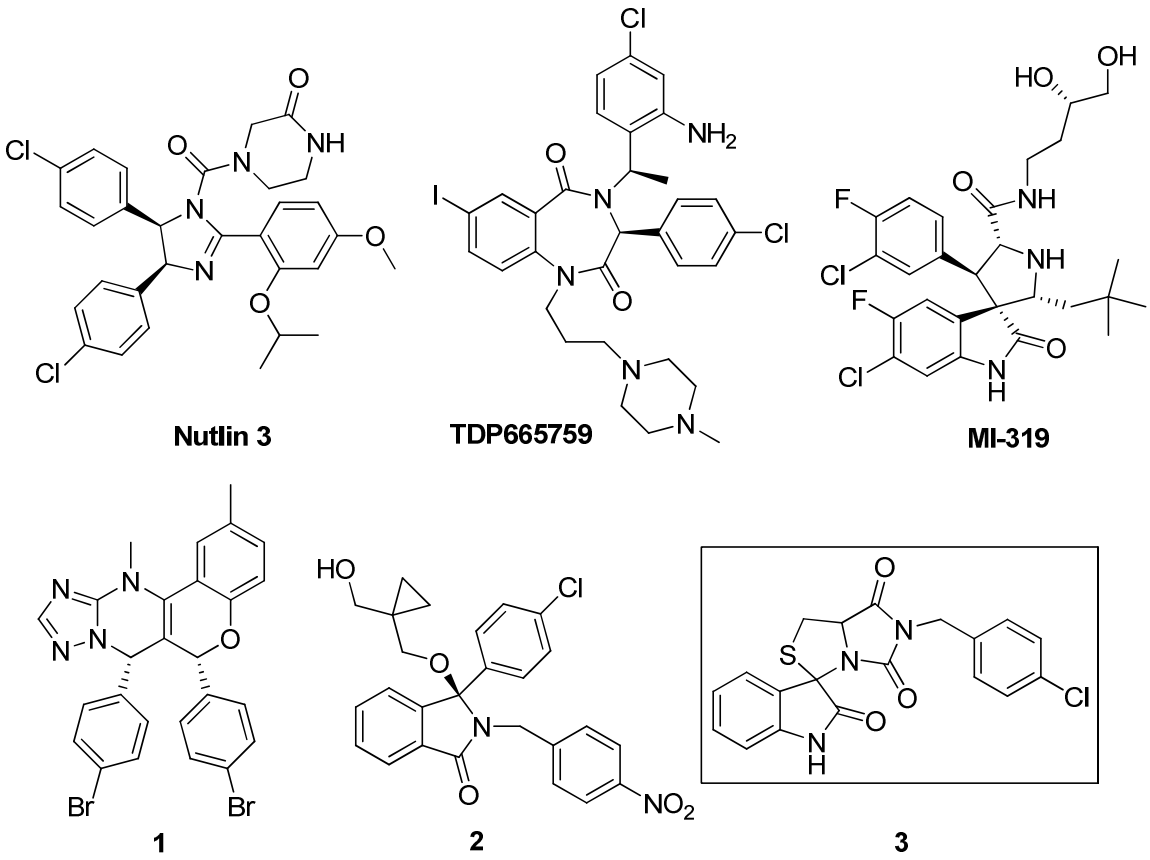

Figure 1. Structure of different inhibitors of p53-MDM2 interaction.

Most of the inhibitors we have described above share a common design of a rigid heterocyclic scaffold highly functionalized with appropriate aryl/alkyl groups, which are supposed to mimic the critical p53 residues that bind MDM2. Different structural studies reveal that the p53-MDM2 protein interaction is mediated by the 15-residue α–helical transactivation domain of p53, which inserts into a hydrophobic cleft on the surface of MDM2.[21] Three residues within this domain, Phe19, Trp23, and Leu26, are essential for MDM2-binding, making this site an attractive target

to design small molecules able to mimic the contacts and the orientations of these key amino acids.[22] Previously, we have reported a series of spiro(oxindole-3,3'-thiazolidine)-based derivatives potentially able to mimic at least two critical p53 residues that bind MDM2.[23] Compound **3** inhibited cell growth of different human tumor cells at submicromolar concentrations (IC_{50} in the range of 0.4-0.9 μM). This derivative induced apoptotic cell death after 24 hrs of treatment at cytotoxic concentrations, but did not alter the normal course of cell cycle. However, **3** induced a time-dependent increment of p53 expression, indicating that the activity profiles of the compound might be regulated by this protein. More concretely, NMR studies performed on compound **3** demonstrated the ability of this compound to block p53-MDM2 interaction. In this paper, we describe the design, synthesis and SAR studies of a more flexible series of spiro(oxindole-3,3'-thiazolidine) derivatives, leading to antiproliferative compounds with significantly improved potency and cellular activity over the parent compounds.

RESULTS AND DISCUSSION

Design

Compound **3** was designed starting from the known spiro-oxindole derivative MI-319 (Figure 1).[23] Its spiro(oxindole-3,3'-thiazolidine) scaffold allows interesting and efficient structural modifications. One of them, opening the imidazole ring, is described in this paper. In fact, we considered it of interest to manipulate the imidazo nucleus of compound **3** with the aim of altering its conformational properties. The opening of this ring would allow us to access more flexible structures (series 4 and 5, Figure 2) with a potential third point of diversification through the 4'-carboxyl group of the thiazolidine moiety. This ring could allow the aromatic and/or alkyl side chains to assume more appropriate orientations to interact with the binding site.

Accordingly, two small libraries of compounds were considered for synthesis. Both series retain the ester group at position C-4' while the oxoindole moiety carries either a weak releasing (CH_3) or a withdrawing (Br) electron groups (R). Series 4 contains a substituted phenyl, benzyl, or a cyclohexyl side chains on the N-3' (R_2), while these groups were positioned on N-1 in the series 5 (R_1).

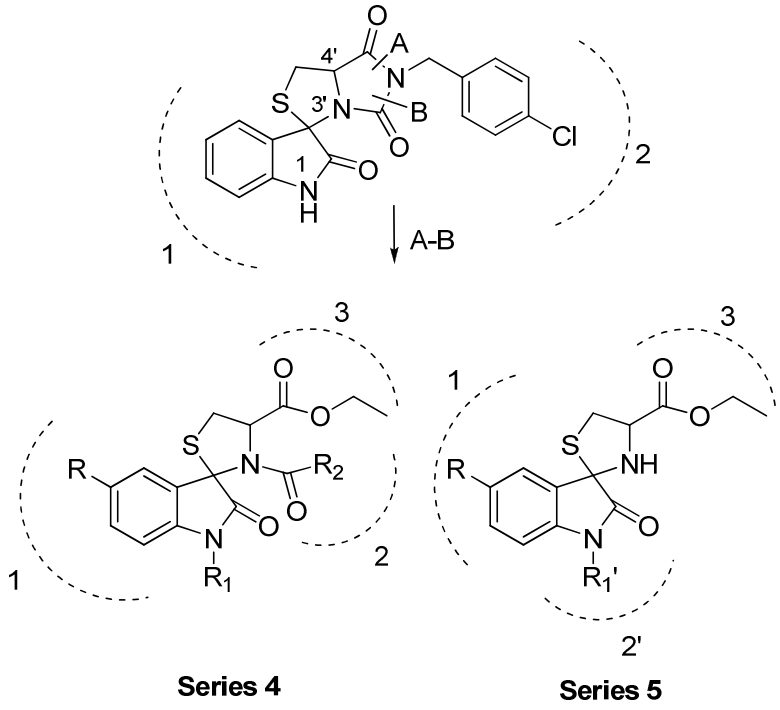

Figure 2. Design of new series 4 and 5. Dashed lines define hypothetical interaction subsites.

Chemistry

The new (2'*R*,4'*R*)-ethyl 3'-substituted-2-oxospiro[indoline-3,2'-thiazolidine]-4'-carboxylate derivatives (**4a-f**, **4l-n**) were prepared applying the synthetic route shown in Scheme 1. Starting spirooxoindolethiazolidine skeletons (**13-18**) were constructed by condensation between the isatin derivatives (**7-12**), and cysteine ethyl ester in EtOH. These derivatives were obtained with 80–90% yields, as (2'*R*)/(2'*S*) epimeric mixtures ranging from 60/40 to 40/60 ratios as we

previously described.[23,24] The 3'-acyl derivatives were obtained by reaction of compounds **13-18** with the corresponding 2-(4-chlorophenyl)acetyl, 4-chlorobenzoyl, 4-methylbenzoyl, benzoyl or cyclohexanecarbonyl chlorides in THF using TEA as base.

Scheme 1.[a] Synthesis of 2-Oxospiro[indoline-3,2'-thiazolidine]-4'-carboxylate Derivatives (series **4** and **5**)

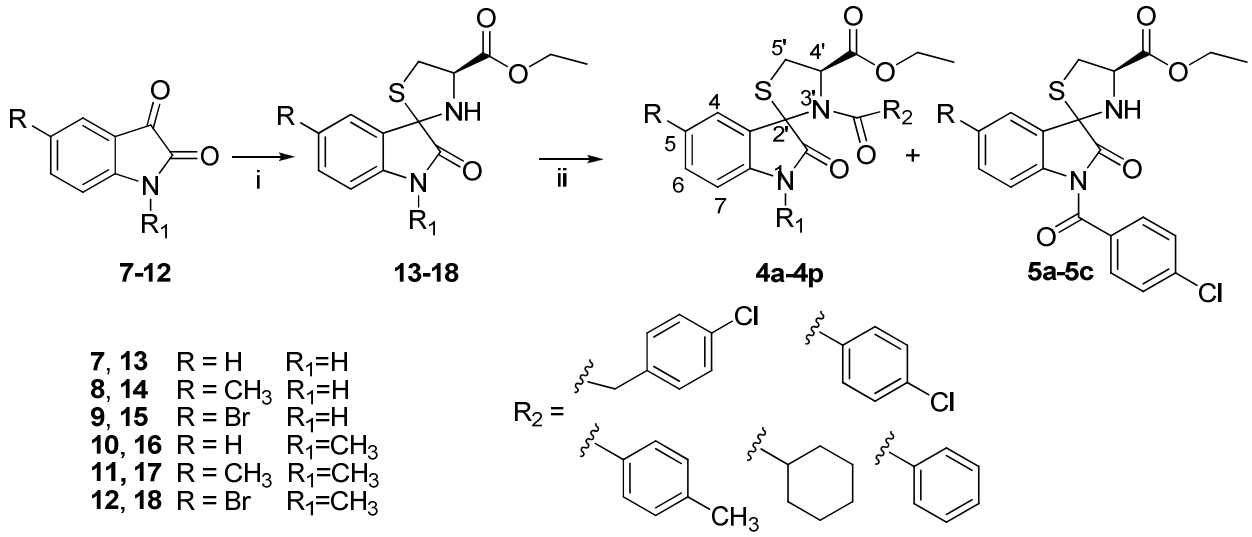

[a] Reagents and conditions: (i) Cys-OEt, $NaHCO_3$ in EtOH; (ii) R_2-COCl, TEA, THF, 2 h, room temp. See Table 1 for the correspondence between number of final products and substituent R, R_1, and R_2.

In these conditions, all final products (**4a-4f** and **4h-4q**) were obtained as single diastereomers in 32-58% overall yields. These stereoselectivity in the acylation reactions of thiazolidine derivatives has been previously observed by us[24] and other authors[25] and can be explained by the fact that thiazolidines undergo facile ring opening and closure reactions. This favors the formation of thermodynamically more stable diastereoisomers. Moreover, the reaction of intermediates **13-15** (R_1 = H) with 4-Cl benzoyl chloride gave also the 1-substituted derivatives

5a-c with 8-12% yields. In the synthesis of the 3-cyclohexylcarboxy derivatives **4n-4q**, two isomers were obtained in a 11/1-6/1 ratio (estimated by ^{1}H NMR), which differ for the *cis/trans* configuration at the N3'-COC_6H_{11} amide bond. The major isomer (*cis*) in these mixtures was identified on the basis of the ROE observed in the ROESY spectrum of **4n** between the H-1" of the cyclohexanecarbonyl group and the H-4' of the thiazolidine (Figure 3 and Figure S1 in Supporting Information). *Cis/trans* isomerization about amide bond was evidenced by 2D NMR.[26] In fact, interconversion was demonstrated by an exchange cross-peak between the H-4' hydrogen signals of the two isomers (Figure S1).

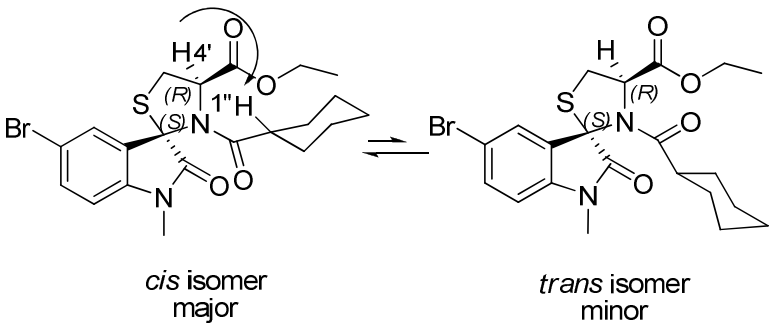

Figure 3. ROE interaction observed between H-4' and H-1" in the ROESY spectrum of compound **4n**.

Changes in the condition of reactions that involve an increase of the reaction time (2h to 12 or 24h) do not significantly modify the above described results, while increase of temperature resulted in a general decrease of reaction yields. However, with the use of microwave (Scheme 2), the reaction of intermediate **15** with 4-chlorobenzoyl chloride led to a mixture of two diastereoisomers (2'*S*, 4'*R*) **4f** and (2'*R*,4'*R*) **4g** and the 1-substituted derivative **5c** in 33, 15, and 9% yields respectively. In the same condition and using cyclohexane carbonyl chloride as acylation agent we observed the formation of only a diastereoisomer (2'*S*, 4'*R*) **4q** (42%), the 1-

cyclohexacarbonyl derivative **5d** (25%), and a minor product with structure of 2-oxo-5'H-spiro[indoline-3,2'-thiazole]-4'-ethyloxycarbonyl **6d** with a 15% yield.

Scheme 2. Reaction of Ethyl 5-bromo-2-oxospiro[indoline-3,2'-thiazolidine]-4'-carboxylate with 4-chlorobenzoyl and cyclohexanecarbonyl chlorides.

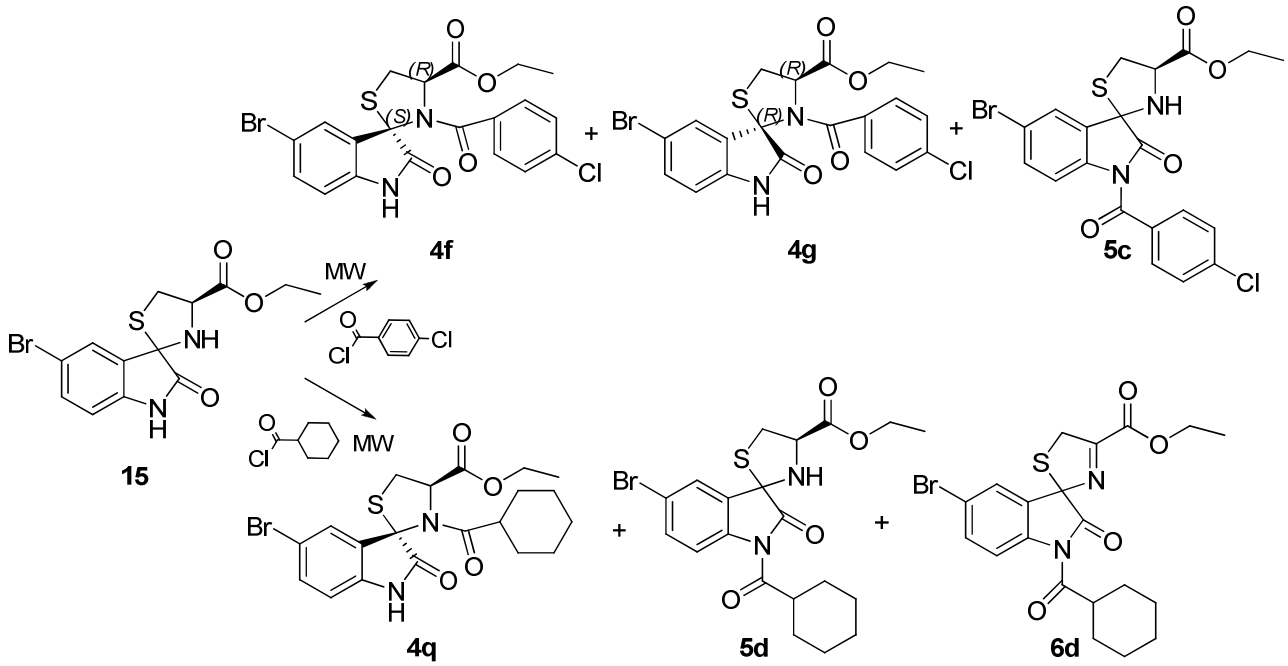

[a] MW. 10 minutes, 100 °C, 2 bar

The assignment of the relative configuration at the C-2' asymmetric center as *R* was determined on the basis of a ROE enhancement between H-4' and H-4 observed in the 2D ROESY spectra of **4g**. Absolute configurations were defined hypothesizing configuration retention at C-4' according to structural determination achieved with the previous series.[23] In contrast, this ROE enhancement was not observed in any of the other derivatives, which were assigned to the *S* stereochemistry at C-2'.

The 1-(4-chlorobenzoyl)-2-oxospiro[indoline-3,2'-thiazolidine] derivatives (**5a-5c**) were prepared using an alternative synthetic route as showed in Scheme 3. Treatment of isatins **7-9** with 4-chlorobenzoyl chloride in DCM and TEA gave the corresponding intermediates **19-21** which were condensed with cysteine ethyl ester in EtOH. In this condition, compounds **5a**-**5c** were obtained as single (2'*S*,4'*R*) diastereoisomer in 60-63% yields according to their 1D and 2D NMR spectra. In addition, working with the 5-substituted intermediates **20** and **21**, we also observed the formation of thiazoline derivatives **6b** and **6c** with 11 and 8% respectively. Moreover, the reaction of **7-9** with cyclohexanecarbonyl chloride did not lead to the desired 1-(cyclohexylcarbonyl) derivative, recovering the starting materials. Poor reactivity of cyclohexane carbonyl chloride could be explained, if compared to 4-chlorobenzoyl chloride, by considering a higher steric hindrance of the first. Modifications of reaction conditions including changes of solvent, increase of temperature or use of microwaves led to the same negative results.

Scheme 3.[a] Synthesis of (2'S,4'R) Ethyl 2-oxospiro[indoline-3,2'-thiazolidine]-4'-carboxylate Derivatives (**5**) and Ethyl 2-oxo-5'H-spiro[indoline-3,2'-thiazole]-4'-carboxylate Derivatives (**6**)

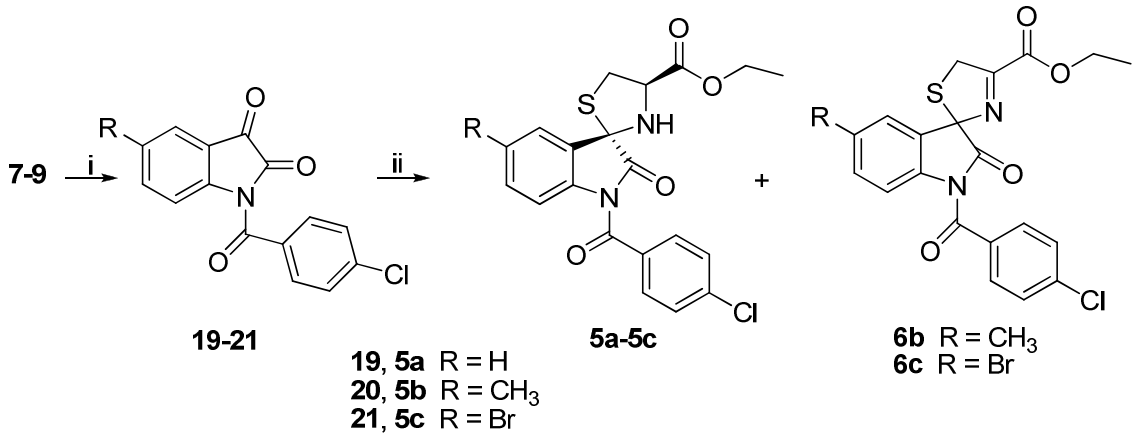

[a] Reagents and conditions: (i) 4-Cl-C_6H_4COCl, TEA, THF, 2 h, room temp. (ii) Cys-OEt, $NaHCO_3$ in EtOH.

BIOLOGICAL EFFECTS

Antiproliferative activity

The spirooxoindolethiazolidine derivatives were examined for antiproliferative activity against two tumor cell lines: the human breast adenocarcinoma MCF-7, and human colon carcinoma HT-29 at 24 hrs. The obtained IC_{50} values are summarized in Table 1.

Table 1. Antiproliferative Activity of Spiro[indoline-3,2'-thiazolidine] (4 and 5) and Spiro[indoline-3,2'-thiazole] (6) Derivatives.

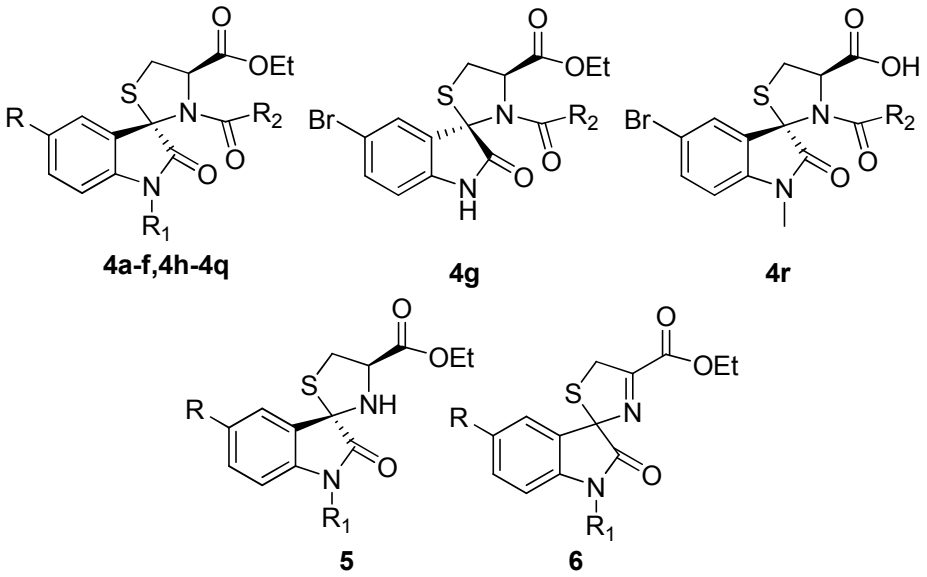

Comp.	R	R_1	R_2	IC_{50} (μM±SD)[a]	
				MCF-7[b]	HT29[b]
3	H	H		1.21± 0.6	1.60 ± 0.4
4a	H	H	$CH_2C_6H_4$(4-Cl)	> 5	1.00±0.2
4b	CH_3	H	$CH_2C_6H_4$(4-Cl)	4.81±1.0	0.78±0.2
4c	Br	H	$CH_2C_6H_4$(4-Cl)	2.90±0.8	0.66±0.1
4d	H	H	C_6H_4(4-Cl)	2.15 ±0.7	3.69±0.9
4e	CH_3	H	C_6H_4(4-Cl)	2.12±0.7	1.09±0.6
4f	Br	H	C_6H_4(4-Cl)	0.90±0.2	0.11±0.09
4g	Br	H	C_6H_4(4-Cl)	3.00 ±0.2	2.00±0.8
4h	H	CH_3	C_6H_4(4-Cl)	4.52±1.1	0.18±0.09
4i	CH_3	CH_3	C_6H_4(4-Cl)	1.23±0.4	0.12±0.07
4j	Br	CH_3	C_6H_4(4-Cl)	0.52±0.3	0.08±0.01
4k	Br	CH_3	$CH_2C_6H_4$(4-Cl)	0.27±0.1	0.36±0.09
4l	Br	CH_3	C_6H_5	0.31±0.1	0.21±0.2
4m	Br	CH_3	C_6H_4(4-CH_3)	0.06±0.05	0.09±0.05
4n	Br	CH_3	Cyclohexyl	0.04±0.01	0.07±0.01
4o	CH_3	CH_3	Cyclohexyl	1.20±0.6	1.10±0.6
4p	H	CH_3	Cyclohexyl	2.30±0.8	1.90±0.8
4q	Br	H	Cyclohexyl	0.22±0.1	0.56±0.1
4r	Br	CH_3	Cyclohexyl	2.01±0.9	1.90±0.7
5a	H	COC_6H_4(4-Cl)	H	1.01±0.6	1.03±0.8
5b	CH_3	COC_6H_4(4-Cl)	H	3.46±0.9	0.23±0.1
5c	Br	COC_6H_4(4-Cl)	H	0.15±0.1	0.02±0.01
5d	Br	Cyclohexyl	H	2.08±0.8	1.40±0.8
6b	CH_3	COC_6H_4(4-Cl)		2.78±0.9	0.21±0.1
6c	Br	COC_6H_4(4-Cl)		0.86±0.4	0.20±0.1
6d	Br	Cyclohexyl		1.63±0.6	0.85±0.4

[a] Data represent mean values (SD) of three independent determinations. [b] Human breast adenocarcinoma cell line. [c] Human colon carcinoma cell line.

Compound **3,** considered our hit compound, showed a similar micromolar antiproliferative activity against the two tumoral cell lines used in the assay. The opening derivatives **4a**, **4b** and **4c** showed an elevated activity with IC_{50} values in the μM range against MCF-7 and submicromolar against HT29 cell lines. Exchange of the 4-chlorobenzyl group for 4-chlorophenyl gave compounds **4d-4f**, more active against MCF-7 cells while **4f** was 6-fold more active against the HT29 cell line. The activity data for compounds **4a-4c**, **4d-4f**, and **4h-4j** (IC_{50} from 0.08 to > 4.0 μM) indicated that the nature of the substituents on the oxoindole moiety markedly affects the anti-proliferative activity profile of these compounds. Contrary to what was observed in the precedent series (compound **3**),[23] the presence of an electron-withdrawing group, such as the bromide group, at position C-5 of the indole system caused an increase of the activity of the corresponding analogues **4c**, **4f**, and **4j** in both cell lines, but, particularly on HT29 cells. We observed that the configuration at the 2' carbon has a notable influence on the cytotoxic activity on this cell line. In fact, (2'*R*, 4'*R*) **4g** was 18-fold less potent than its diastereoisomer (2'*S*, 4'*R*) **4f** on HT29 cells, and 3-fold less potent on the MCF-7 cell line. The introduction of a methyl group at N-1 improved the activity of compounds **4h-j** compared to the non-methylated analogues (**4d-f**), specially on colon cell line. The most potent compound of this subseries, **4j**, gave IC_{50} values of 520 and 80 nM in MCF-7 and HT29 cell lines, respectively. Modifications of **4j** at the N-3'position produced different effects: the introduction of 4-Cl-benzyl group increased (2-fold) the antiproliferative activity of analogue **4k** on MCF-7 cells and reduced (4-fold) its activity on HT29 cells. A similar behavior was observed with the compound **4l** which contains a

phenyl group at N-3' position. The introduction of a 4-CH_3-phenyl or a cyclohexyl group led to compounds **4m** and **4n**, which showed an anti-proliferative activity in the nanomolar range (IC_{50} < 100 nM, for both cell lines). In particular, **4n** was 14-fold more potent than its analogue **4j** on MCF-7 cells. Further modifications of this compound involving substitution or loss of the Br atom at the C5 (compounds **4o** and **4p**), lack of the CH_3 group at N1 (compound **4q**), as well as ethyl ester hydrolysis to carboxylic acid (**4r**), all resulted in a loss of activity in the resulting compounds. These derivatives were less potent than **4n** against MCF-7 (from 5- to 60-fold) and HT29 (from 8- to 28-fold) cell lines.

Furthermore, switching the 4-Cl-benzoyl or cyclohexyl carbonyl groups from position N3' to position N1 led to contrasting results. 4-chlorobenzoyl derivative **5c** showed cytotoxic activity in the nanomolar range on both cell lines (IC_{50} = 150 and 20 nM) and was ~ 6 fold more potent than its regioisomer **4f**. Derivative **5a** was also 2-3 fold more potent than its regioisomer **4d**, while compound **5b** containing a CH_3 group at C-5 position showed a slight decrease of activity on MCF-7 cells compared to its analogue **4e**. In contrast, compound **5b** was 4-fold more potent than **4e** against HT29 cells. Surprisingly, the same change of the position for cyclohexyl carbonyl group (**4q** versus **5d**) led to a considerable decrease in activity. In fact, **5d** was 10-fold less potent than its regioisomer **4q** on MCF-7 cells. Finally, the presence of a more planar thiazoline ring in the structure produced different effects: derivative **6b** retained the cytotoxic activity of its thiazolidine analogue **5b**, while compound **6c** was 6- and 10-fold less active than **5c** on both cell lines. In contrast, compound **6d** showed a slight increase of activity (~1.5 fold) on both cell lines compared to **5d**.

The anti-proliferative activity of the most potent compound against both cell line, **4n**, was also analyzed against a panel of human tumor cell lines, including PC3 (prostate), U937 (leukaemia),

Calu (lung), HEPG2 (liver), and C643 (anaplastic thyroid) human cell lines (Table 2). Doxorubicin and Nutlin-3 were used as reference cytotoxic agents. Also data on the MCF-7 cell line are reported in Table 2. In all tested cells lines, compound **4n** showed marked cytotoxic potency with IC_{50}s in the range 0.07-0.55 μM, while Nutlin-3 was much less effective in our panel in accordance with some data found in the literature.[27] **4n** was 18-fold more potent than doxorubicin on the Calu cell line and was equipotent to doxorubicin in PC3 and U937 cell lines.

Table 2. Antiproliferative Activity of **4n** on Multiple Human Tumor Cell Lines and One Normal Cell Line.

		IC_{50} (μM±SD)		
Origin tumour	Cell line	**4n**	Nutlin-3	Dox
Breast	MCF-7	0.04±0.01	2.9±0.31[27a]	0.02±0.01
Prostate	PC3	0.41±0.21	30.3±2.9[27b]	0.75±0.10
Leukemia	U937	0.07±0.01	15.6±1.9	0.12±0.03
Lung	Calu	0.10±0.06	27.2±5.3	1.81±0.33
Liver	HEPG2	0.14±0.06	10.2±5.1[27c]	0.08±0.01
Anaplastic Thyroid	C643	0.55±0.08	23±11.2	0.07±0.01
Origin normal				
Human Gingival Fibroblast	HGF	1.60±0.15	1.40±3.6	0.50±0.15

[a] Data represent mean values (SD) of three independent determinations at 24 hrs.

Table 2 also shows that **4n** inhibited the cellular growth of a human gingival fibroblast (HGF) normal cell line at low micromolar concentration. This cytotoxicity was similar to that showed by Nutlin-3 on the same line and was 4 times less than that caused by doxorubicin. These data seem to indicate that **4n** has a good profile of cell selectivity.

In vitro modulation of p53-MDM2 interaction

In order to test the ability of **4n** to inhibit p53-MDM2 interaction we performed an in vitro binding assay using ImmunoSet™ p53/MDM2 complex ELISA (Figure S4). Nutlin-3 and compound **3** were also evaluated as references. In this assay and for all compounds, the minimum effective concentration was determined at 5 μM. At this concentration, the percentage inhibition was 19% for Nutlin-3 and 25% for **3**, while compound **4n** has proved more effective inhibiting 30% of p53-MDM2 interaction.

Molecular Modeling studies

To better rationalize the reasons behind the activity of our indoline-3,2'-thiazolidines molecular docking studies were undertaken on **4n** which is the most potent antiproliferative agent in this series. To date, several X-ray structures are reported of the complex between MDM2 and different small molecules and, among these, we decided to choose the structure having PDB code 1LBL[28] in which MDM2 was solved at a very high resolution (1.60 Å) in complex with a spiro-oxindole derivative that is structurally related with the derivatives described herein. Therefore, this structure was used to dock, through the Autodock4.2 (AD4) software,[29] compound **4n** as well as the co-crystal ligand. Docking of the latter compound confirmed the good performances of this software which was able to predict the experimental binding pose with a root-mean square

deviation (rmsd) of 1.03 Å. In regards to **4n,** the same calculations converged towards a single solution in which the lowest energy (ΔG_{AD4}) binding conformation was also belonging to the most populated cluster (f_{occ}). In particular, in the binding pose (ΔG_{AD4}= -8.32 kcal/mol, f_{occ}=86/100) predicted for **4n** (Figure 4) the ligand is inserted in the MDM2 binding site so that the 3-cyclohexylcarboxy substituent is buried in the so-called Trp23 pocket making favorable van der Waals contacts with Ile61, Val75, Phe86, Phe91 and Ile99 side-chains. On the other hand, the MDM2 Phe19 subpocket is occupied by the ligand ethyl ester chain that is able to make direct contacts with Ile61 and Met62 side-chains. The presence of this interaction could partially explain why hydrolysis of the ethyl ester chain to the corresponding carboxylic acid results in the loss of activity, on the other hand, reduction of membrane penetration cannot be ruled out. Interestingly, the Leu26 cleft does not seem to be completely filled by the 5-bromo-2-oxoindoline nucleus that, instead, forms additional hydrophobic interactions with Leu54 through its N1-methyl substituent. This latter hydrophobic interaction could explain why **4d-f** are generally less active than their methylated analogues **4h-j**. In this position, edge-face π–π interaction with the Phe55 residue are also established in a shallow and rather liphophilic portion of the MDM2 protein in which the 5-bromine atom fills the crevice between Phe55, Met62, and Gln59. Indeed, the interaction with Phe55 residue has already been detected through X-ray studies for other structurally unrelated ligands in a very recent work by Olson's group[30] Interestingly, in the binding pose suggested by AD4 the ligand N3'-COC_6H_{11} amide bond adopts a *cis* configuration as already suggested by ROESY experiments.

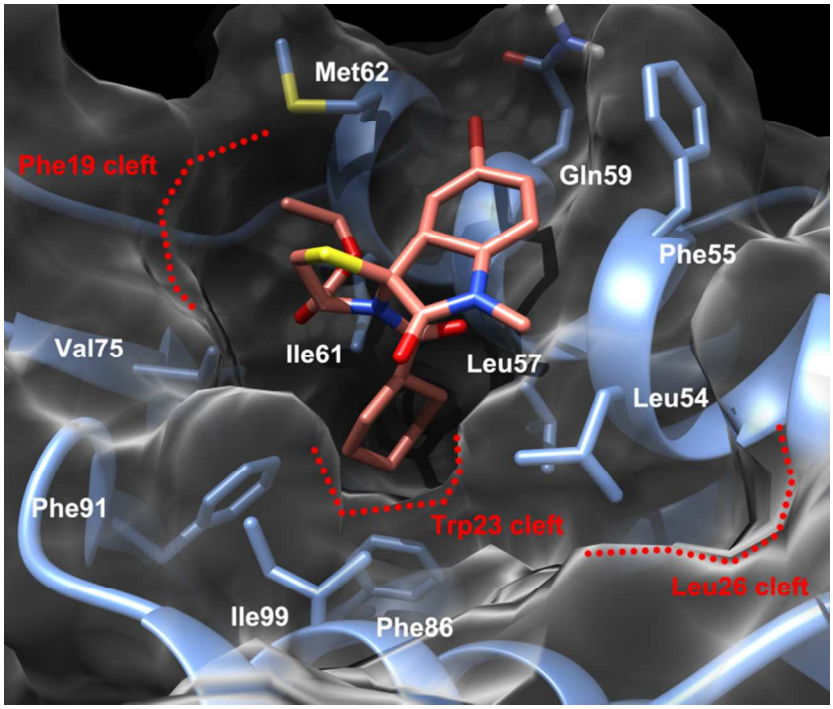

Figure 4. Predicted binding mode for compound **4n** in the MDM2 binding site. The ligand is represented as pink stick while the protein as blue sticks and ribbons and transparent white surface.

Modulation of p53-MDM2 interaction in cell

To confirm in cell the ability of **4n** to inhibit the MDM2-p53 interaction, the expression levels of these two proteins were evaluated by western blot after 24, 48 and 72 hrs of **4n** treatment and after 24 hrs with Nutlin-3. Compound concentrations close to their IC_{50} on the MCF-7 cell line were used in this assay (i.e., 50 nM for **4n** and 3 μM for Nutlin-3). In these conditions, **4n** induced the accumulation of p53 and MDM2 proteins, (Figure 5A and 5B). To determine whether **4n** was able to prevent MDM2-p53 interaction, p53 expression levels were measured after MDM2 immunoprecipitation (Figure 5C and 5D). Cells were treated with **4n** for 24, 48, and 72 hrs or Nutlin-3 for 24 hrs. MDM2 was immunoprecipitated and the samples underwent western blot to visualize p53, and evaluate its association with MDM2. Treatment with **4n**

reduced the MDM2-p53 interaction as evidenced by a significant decrease in the p53 levels bound to MDM2 at 24 and 48 hrs. Nutlin-3 seems to be inactive in this immunoprecipitation assay. We can hypothesize that Nutlin acts more quickly than **4n**; its unresponsiveness to the test may be due to a recombination of p53 and MDM2 within 24 hrs. Interestingly, this recombination is also observed for **4n** after 72 hrs.

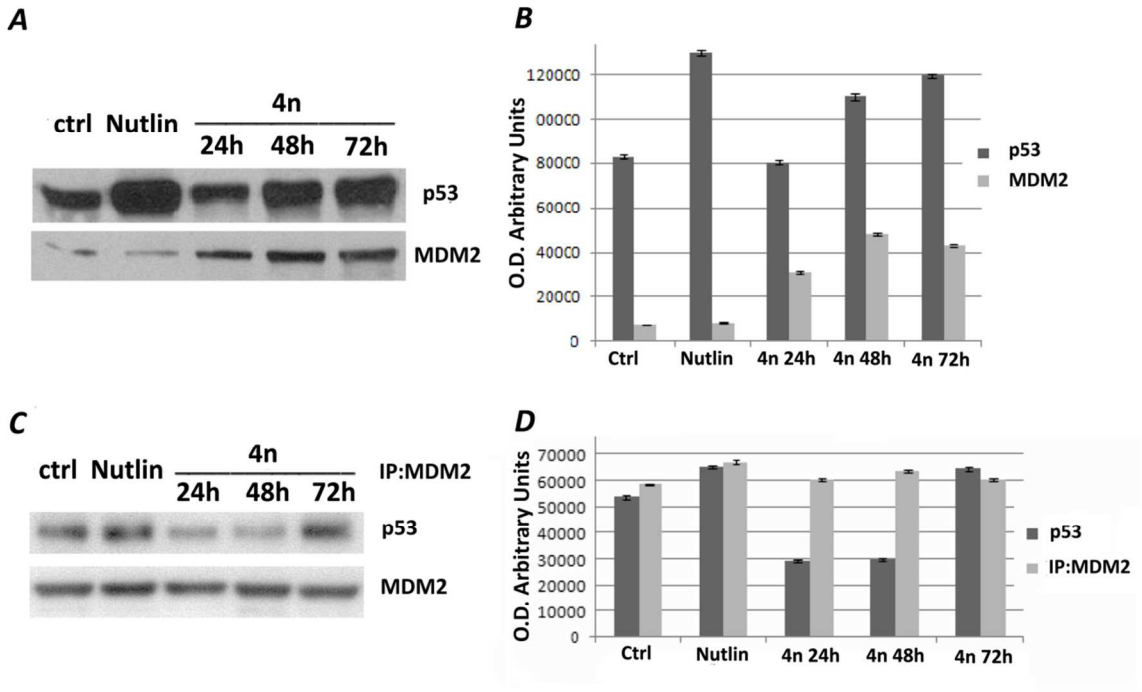

Figure 5. (A) MCF-7 cells were treated with 50 nM **4n** for 24, 48 and 72 hrs or 3 μM Nutlin-3 for 24 hrs. Total cell lysates were analyzed by western blotting for p53 and MDM2 with specific antibodies. (C) A similar experiment was performed for p53 after MDM2 immunoprecipitation. (B and D) Immunoblots were quantified by ImageQuant densitometric analysis. Protein expression levels were measured in arbitrary densitometric units and data show the means ± SEM calculated from relative protein expression levels determined in three separate experiments.

Cell-cycle progression

To investigate the effect in the reduction of tumor cell survival mediated by **4n**, MCF-7 cell cycle was analyzed after 24, 48 and 72 hrs of treatment. Again, Nutlin-3 was used for comparison. Nutlin-3 (3 μM) induced cell cycle arrest, as shown by G0/G1 phase block, and in accordance with literature data.[16] Compound **4n** (50 nM) did not significantly affect cell cycle. Indeed, **4n**-treated cells showed the same distribution in G1, S, G2/M phases of untreated cell at 24, 48 or 72 hrs (Figure 6A, 6B, and 6C). When the same experiment was performed with increasing concentration of **4n** (500 nM, 1 μM, 5 μM), no difference in cell cycle effect was found compared to initial concentration (Figure 6 D).

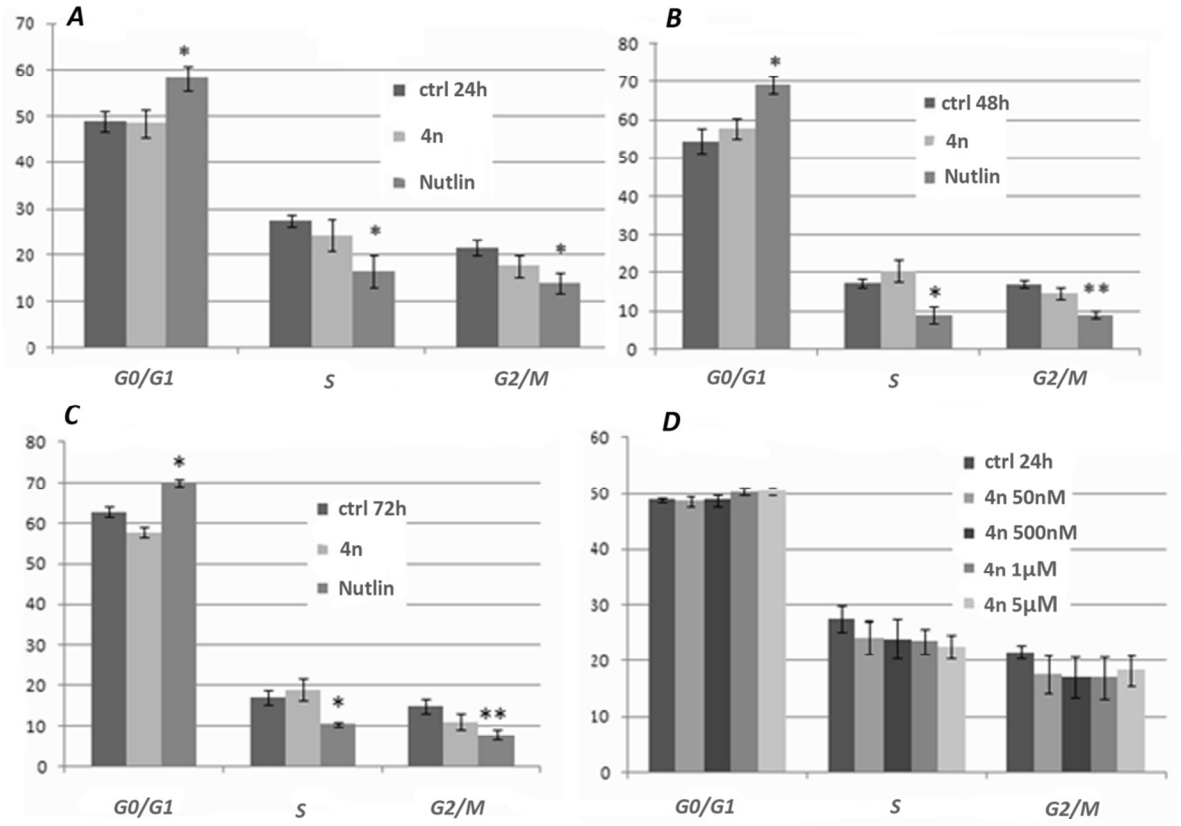

Figure 6. Effects of **4n** on cell cycle progression analyzed for DNA content by FACS in breast cancer MCF-7 cells untreated or treated with 50 nM **4n** or 3 μM Nutlin-3 at 24 (A), 48 (B) and 72 hrs (C) and (D) MCF-7 cells untreated or treated with 50, 500, 1000 and 5000 nM of **4n** at

24 hrs. The distribution and percentage of cells in G1, S and G2/M phase of the cell cycle are indicated. Data points are means SEM. Significance assumed at *$p<0.05$, **$0.01<p<0.05$, ***$p<0.01$

Apoptotic cell death

Cell death was evaluated with preliminary, qualitative assessment of apoptosis by subG1 analysis. The treatment with **4n** (50 nM) showed a strong increase of the subG1 peak, that rose in a time dependent manner (Figure 7A). Nutlin-3 (3 μM) also induced a significant increase of cell death. However, the subG1 peak may consist of apoptotic and necrotic cells: to discriminate between the two possibilities, an annexin V binding assay was performed. **4n** and Nutlin-3 induced a significant increase of cell fraction in early apoptosis (Figure 7B). In particular, the apoptotic cell percentage increased from 4% of untreated cells to 10% and 12% of cells after 48 and 72 hrs of **4n**-treatment. Nutlin-3 determined a lower increase of early apoptosis compared to **4n**.

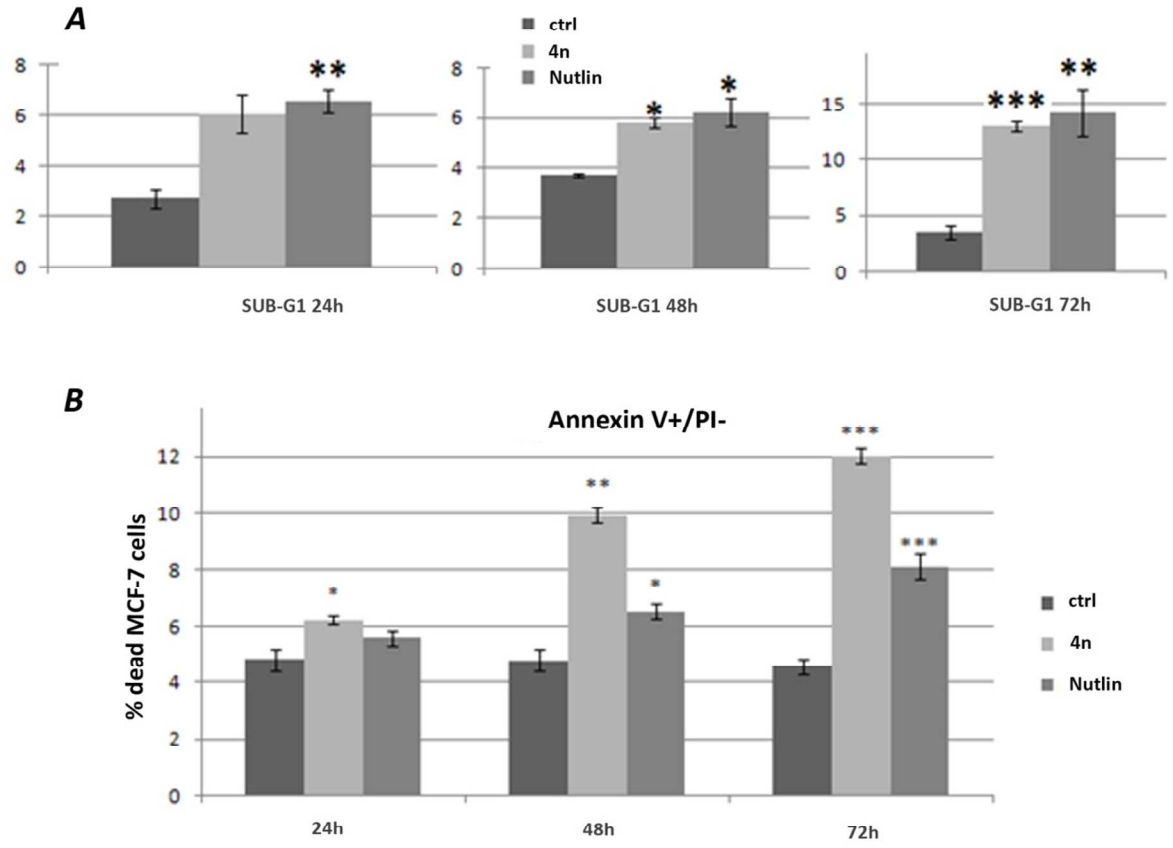

Figure 7. (A) Representative subG1 populations calculated from FACS histograms. MCF-7 cells were incubated with 50 nM **4n** or with 3 μM Nutlin-3 for 24, 48 and 72 hrs. Data are expressed as the percentage of subG1 cells. (B) A similar experiment was performed and the cells were analysed by FACS for the occurrence of apoptosis (FITC-annexin binding). Values represent the mean ± SEM. Significance assumed at *$p<0.05$, **$0.01<p<0.05$ ***$p<0.01$

Although p53 plays a pivotal role in regulating cell cycle and apoptosis,[2,3] treatment of MCF-7 cells with **4n** or Nutlin-3 has a different impact on both mechanisms. Indeed, whereas Nutlin-3 determined a cell cycle arrest, **4n** induced apoptotic cell death. To investigate the cell death mechanism induced by **4n**, the p53-dependent apoptotic pathway was analyzed by Western blot. The analysis of the expression levels of p53 and p53 transcriptional targets, such as p21 and p27, showed a progressive increase of these proteins during the treatment with **4n** in a time dependent

manner (Figure 8). However, these increases do not seem to be sufficient to induce cell cycle arrest. On the contrary, Nutlin-3 showed a greater accumulation of p21 than **4n**, at 24, 48 and 72 hrs, inducing cell cycle arrest (Figure 8A and 8B). Cells committed to die via p53-dependent apoptosis typically follow the mitochondrial pathway, although p53 can also modulate cell death through death receptors.[31,32] p53 has been reported to trigger apoptosis by modulation of gene transcription of Bcl2 family members and by physical interaction with these proteins.[31-33] Western blot results indicated that **4n** and Nutlin regulate Bcl-2 members, reducing the anti-apoptotic Bcl-xL protein and increasing the pro-apoptotic Bcl-xS protein, although the two drugs affect BclxL/S expression at different times.

.

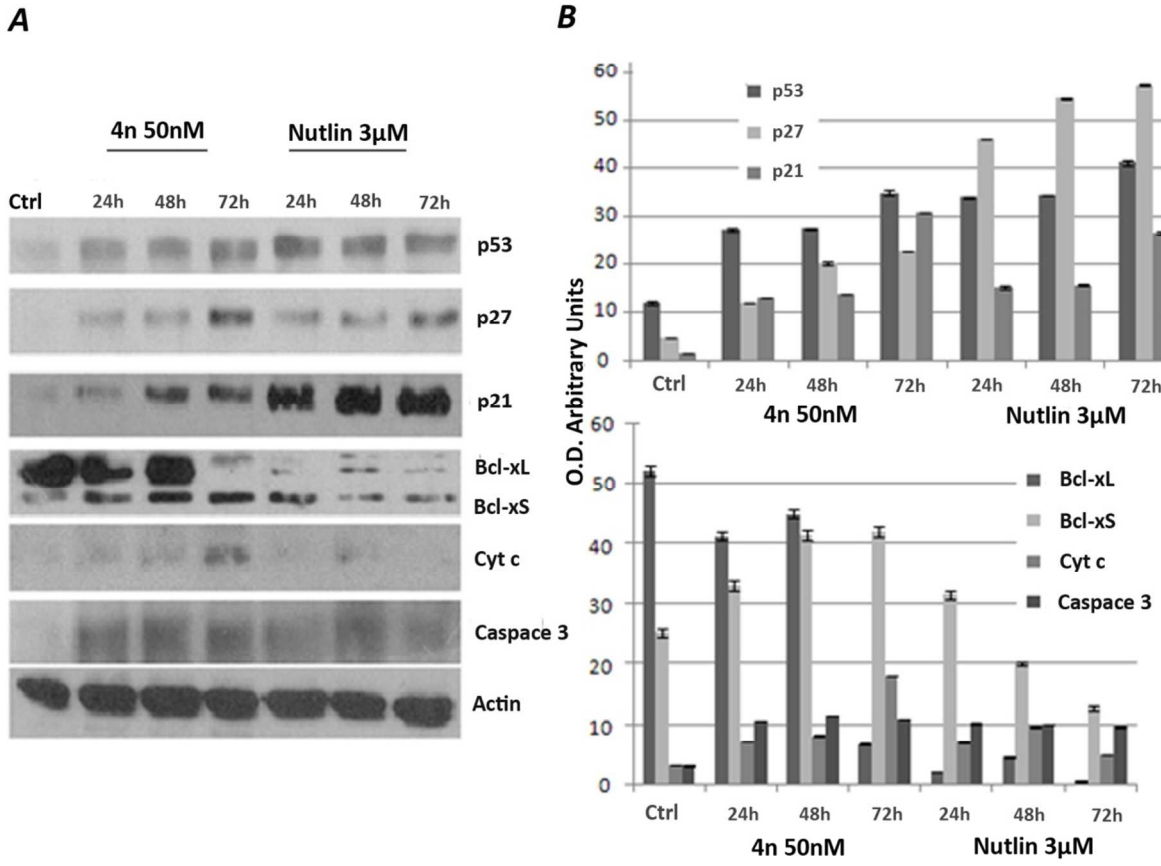

Figure 9. (A) MCF-7 cells were treated with 50 nM **4n** or 3 μM nutlin for indicated time interval. Total cell lysates were analyzed by western blotting for phosphotyrosine p53, p21, p27, Bcl-xL/xS, cytocrome c and caspase-3 with specific antibodies. (B) Immunoblots were quantified by ImageQuant densitometric analysis. Protein expression levels were measured in arbitrary densitometric units and data show the means ± SEM calculated from relative protein expression levels determined in three separate experiments. *$p<0.05$ vs protein expression levels in untreated control cells.

The induction of **4n**-mediated apoptosis was confirmed by the release of cytochrome c from mitochondria to the cytosol, that increased at various time intervals becoming particularly evident at 72 hrs of drug treatment. Also Nutlin-3 affects cytochrome c release at 48 h even if at lower levels compared to **4n**.[34,35] One of the final effectors of the apoptotic process is caspase-3, that is activated both by extrinsic and intrinsic or mitochondrial pathways. The cleavage of caspase-3 is a clear indicator of apoptosis, hence we analyzed the p53-fragment with a specific antibody. Western blot analysis revealed that both **4n** and Nutlin-3 induced an accumulation of the cleavage product of caspase-3. All these finding suggest that, in the MCF-7 breast cancer cell line, cell cycle arrest is the main molecular mechanism mediated by Nutlin-3. On the contrary, 50nM **4n** did not block cell cycle progression but rather it induced apoptosis.

CONCLUSIONS

Here we report the synthesis, and biological evaluation of a series of new 2-oxospiro[indoline-3,2'-thiazolidine] derivatives, designed as inhibitors of p53-MDM2 protein-protein interaction, which exhibit activity against different tumor cell lines. In particular, compound **4n** showed high efficacy in MCF-7 (breast), HT29 (colon), calu (lung), and U937 (leukemia) human cell lines with IC_{50} values of 40, 70, 100, and 70 nM, respectively, with >10-fold selectivity against the HGF normal cell line. The well known p53-MDM2 inhibitor, Nutlin-

3, was considerably less efficient in all tested cell lines and also in the in vitro p53-MDM2 binding inhibition assay. Docking studies allow us to predict binding mode for **4n** in the MDM2 binding site, in which our compound sets favorable van der Waals contacts with Ile61, Val75, Phe86, Phe91 and Ile99 side-chains, direct contacts with Ile61 and Met62 side-chains, and additional hydrophobic interactions with Leu54 and edge-face π–π interaction with the Phe55 residue. In the MCF-7 cell line, **4n** induces a time-dependent increment in p53 expression, indicating that its activity profile, as in the case of nutlins, might be regulated by this protein. However, preliminary studies on the induction of apoptosis and cell cycle progression, showed a different behavior for these compounds. Nutlin-3 markedly blocked the G0/G1 phase, causing a delay of cell cycle progression in responsive cells, while treatment with **4n** did not alter the normal course of cell cycle. Moreover, **4n** induces apoptotic cell death through the intrinsic apoptotic pathway. According to these findings, **4n** represents a new lead compound for the design of agents able to reactivate p53-mediated apoptosis in cancer cells and provides a new tool for studying p53 signaling in the natural cellular context of tumors that retain wild-type p53. Further experiments aimed to identify more potent spirothiazolidin-based derivatives and to better understand the apoptotic mechanisms induced by this compound are underway.

EXPERIMENTAL SECTION

General. Reagents, starting materials, and solvents were purchased from commercial suppliers and used as received. Analytical TLC was performed on plates coated with a 0.25 mm layer of silica gel 60 F254 Merck and preparative TLC on 20 cm x 20 cm glass plates coated with a 0.5 mm layer of silica gel PF254 Merck. Silica gel 60 (300-400 mesh, Merck) was used for flash chromatography. Melting points were determined by a Kofler apparatus and are uncorrected.

Optical rotations were measured on an Atago Polax 2-L polarimeter. ^{1}H NMR and ^{13}C NMR spectra were recorded with a Varian-400 spectrometer, operating at 400 and 100 MHz, respectively. Chemical shifts are reported in δ values (ppm) relative to internal Me_4Si, and *J* values are reported in hertz (Hz). ROESY[36] experiment was recorded at 25 °C in the phase-sensitive mode using the method from States.[37] Data block sizes were 2048 addresses in t2 and 512 equidistant t1 values. Before Fourier transformation, the time domain data matrices were multiplied by shifted sin2 functions in both dimensions. A mixing time of 500 ms was used. ESIMS experiments were performed on an Applied Biosystem API 2000 triple-quadrupole spectrometer. Starting spiro(oxoindolethiazolidine) ethyl ester derivatives (**13**-**18**) were synthesized as described in references 23 and 24. As example, here we described the synthesis of (3RS,4'R)-ethyl 5-bromo-1-methyl-2-oxospiro[indoline-3,2'-thiazolidine]-4'-carboxylate (**18**). Combustion microanalyses were performed on a Carlo Erba CNH 1106 analyzer, and all reported values are within 0.4% of calculated values (Table 1S in Supporting Information). These elemental analyses confirmed >95% purity.

Synthesis of (3RS,4′R) ethyl 5-bromo-1-methyl--2-oxospiro[indoline-3,2′-thiazolidine]-4′-carboxylate (18).

$NaHCO_3$ (1.0 g, 12 mmol) and 5-bromo-1-methyl isatin (**12**, 2.4 g, 10 mmol) were added to a solution of *L*-Cys-OEt (2.3 g, 12 mmol) in ethanol (100 mL) and the suspension was stirring at room temperature for 12 h. Then, the suspension was filtered and the filtrate was concentrated. Spiro(oxoindolethiazolidine) ethyl ester residue was dissolved in DCM and washed with water (3 x 50 mL). The combined organic layer was dried over anhydrous sodium sulfate, filtered, and concentrated. A 5:1 diastereoisomeric mixture of the title's compound was obtained, as oil with 73% yied. ^{1}H NMR (400 MHz, $CDCl_3$) δ 1.36 (3H, m, C*H*$_3$), 3.10 and 3.12 (3H, s, C*H*$_3$), 3.31

and 3.43 (1H, m, H-5'a), 3.71 and 3.93 (1H, m, H-5'b), 4.25 (4H, m, CH_2), 4.46 and 4.66 (2H, m, H-4'), 6.69 and 6.75 (1H, d, *J* = 8.0 Hz, H-7), 7.48 (1H, d, H-6), 7.60 and 7.71 (1H, s, H-4).The compound was used in the next reaction without further purification

General Procedure for the Synthesis of the (2'*R* o 2'*S*, 4'*R*)-ethyl 3'-substituted-2-oxospiro[indoline-3,2'-thiazolidine]-4'-carboxylate Derivatives (4a-q). To a solution of (2'*R*,4'*R*)- and (2'*S*,4'*R*)-ethyl 2-oxospiro[indoline-3,2'-thiazolidine]- 4'-carboxylate derivatives (**13-18**, 200 mg, 5 mmol) in dry THF (50 mL) was added a solution of corresponding 4-chlorobenzoyl or 4-methylbenzoyl or 4-chlorophenylacethyl or cyclohexane carbonyl chlorides (5.5 mmol) in THF (10 mL) and TEA (10 mmol). The reaction mixture was stirred at room temperature for 2 h and water was then added. The organic solution was washed with water (3x 100 mL), dried over Na_2SO_4, and evaporated in vacuo. Flash chromatography on silica gel, using ethyl acetate/n-hexane as eluent, overall yielded the correspondent final derivatives as oil.

(2'*S*,4'R)-ethyl 3'-(2-(4-chlorophenylacetyl)-2-oxospiro[indoline-3,2'-thiazolidine]-4'-carboxylate (4a)

Overall yield 43%. $[\alpha]^{25}_D$ -7.1 (c 0.1, MeOH). ^{1}H NMR (400 MHz,$CDCl_3$) δ 1.40 (t, 3H, CH_3); 3.44 (d, 1H, *J* = 12.0 Hz, H-5'a); 3.63 (s, 2H, CH_2); 3.95 (dd, 1H, *J* = 6.0 and 11.6 Hz, H-5'b); 4.39 (q, 2H, CH_2); 5.08 (d, 1H, *J* = 6.0, H-4'); 6.76 (d, 1H, *J* = 8.4 Hz, H-7); 7.04 (t, 1H, H-6); 7.15 (d, 2H, *J* = 8.0 Hz, aryl); 7.24 (t, 1H, *J* = 7.9 Hz, H-5); 7.28 (d, 2H, aryl); 7.43 (s, 1H, NH); 7.47 (d, 1H, H-4). ^{13}C NMR (100 MHz,$CDCl_3$) δ 14.5 (*C*H_3), 34.6 (C-5'), 41.4 (*C*H_2), 62.5 (*C*H_2), 64.3 (C-4'), 73.9 (C-2'), 109.3, 115.8, 123.5, 128.0, 128.9, 130.2, 134.4, 136.2, and 143.1 (aryl), 170.1, 173.9, and 178.0 (C=O). ESIMS m/z calcd for $C_{21}H_{19}ClN_2O_4S$, 430.08; found 430.16.

(2'*S*,4'*R*)-ethyl 5-methyl-3'-(2-(4-chlorophenyl)acetyl)-2-oxospiro[indoline-3,2'-thiazolidine]-4'-carboxylate (4b)

Overall yield 39%.$[\alpha]^{25}_{D}$ -13.6 (c 0.25, MeOH). ^{1}H NMR (400 MHz,$CDCl_3$) δ 1.42 (t, 3H, CH_3); 2.04 (s, 3H, CH_3); 3.37 (d, 1H, *J* = 12.4 Hz, H-5'a); 3.61 (s, 2H, CH_2); 3.98 (dd, 1H, *J* = 6.0 and 11.6 Hz, H-5'b); 4.43 (q, 2H, CH_2); 5.04 (d, 1H, *J* = 6.0, H-4'); 6.70 (d, 1H, *J* = 8.0 Hz, H-7); 7.08 (d, 1H, H-6); 7.19 (d, 2H, *J* = 8.0 Hz, aryl); 7.31 (d, 2H, aryl); 7.40 (s, 1H, H-4); 7.79 (s, 1H, NH). ^{13}C NMR (100 MHz,$CDCl_3$) δ 14.2 (*C*H_3), 21.7 (*C*H_3), 34.8 (C-5'), 41.6 (*C*H_2), 62.3 (*C*H_2), 64.7 (C-4'), 74.2 (C-2'), 109.8, 123.2, 128.5, 129.6, 130.7, 133.0, 137.4, and 142.8 (aryl), 170.6, 173.4, and 178.3 (C=O). ESIMS m/z calcd for $C_{22}H_{21}ClN_2O_4S$, 444.09; found 444.15.

(2'*S*,4'*R*)-ethyl 5-bromo-3'-(2-(4-chlorophenyl)acetyl)-2-oxospiro[indoline-3,2'-thiazolidine]-4'-carboxylate (4c)

Overall yield 37%. $[\alpha]^{25}_{D}$ -29.4° (c 0.4, MeOH). ^{1}H NMR (400 MHz,$CDCl_3$) δ 1.43 (t, 3H, CH_3); 3.42 (d, 1H, *J* = 12.6 Hz, H-5'a); 3.65 (s, 2H, CH_2); 4.01 (dd, 1H, *J* = 6.0 and 12.0 Hz, H-5'b); 4.45 (q, 2H, CH_2); 5.00 (d, 1H, *J* = 6.0, H-4'); 6.73 (d, 1H, *J* = 7.6 Hz, H-7); 7.23 (d, 2H, *J* = 8.0 Hz, aryl); 7.31 (d, 2H, aryl); 7.48 (d, 1H, H-6); 7.95 (s, 1H, H-4); 8.04 (s, 1H, NH). ^{13}C NMR (100 MHz,$CDCl_3$) δ 14.3 (*C*H_3), 21.9 (*C*H_3), 34.6 (C-5'), 41.5 (*C*H_2), 62.4 (*C*H_2), 64.9 (C-4'), 74.4 (C-2'), 109.5, 116.2, 123.4, 128.2, 129.0, 131.1, 132.5, 133.3, 137.2, and 143.2 (aryl), 170.2, 173.5, and 178.9 (C=O). ESIMS m/z calcd for $C_{21}H_{18}BrClN_2O_4S$, 507.99; found 508.04.

(2'*S*, 4'*R*)-ethyl 3'-(4-chlorobenzoyl)-2-oxospiro[indoline-3,2'-thiazolidine]-4'-carboxylate (4d)

Overall yield 49%. $[\alpha]^{25}_{D}$ -16.3 (c 0.25, MeOH). ^{1}H NMR (400 MHz,$CDCl_3$) δ 1.36 (t, 3H, CH_3); 3.40 (d, 1H, *J* = 11.6 Hz, H-5'a); 3.95 (dd, 1H, J = 6.0 and 11.6 Hz, H-5'b); 4.38 (q, 2H,

C*H*$_2$); 4.87 (d, 1H, *J* = 6.0 Hz, H-4'); 6.77 (d, 1H, *J* = 8.0 Hz, H-7); 7.05 (t, 1H, *J* = 7.6 Hz, H-6); 7.20 (t, 1H, H-5); 7.33 (d, 2H, aryl, *J* = 7.6 Hz); 7.44 (d, 2H, aryl); 7.73 (d, 1H, H-4); 8.54 (s, 1H, NH). ^{13}C NMR (100 MHz,$CDCl_3$) δ 14.5 (*C*H$_3$), 34.5 (C-5'), 62.8 (*C*H$_2$), 66.8 (C-4'), 72.4 (C-2'), 110.7, 123.2, 125.5, 126,3, 128.4, 129.0, 130.3, 134.3, 137.1, and 141.2 (aryl), 168.4, 170.6, and 177.1 (C=O). ESIMS m/z calcd for $C_{20}H_{17}ClN_2O_4S$, 416.06; found, 416.14.

(2'*S*,4'*R*)-ethyl 3'-(4-chlorobenzoyl)-5-methyl-2-oxospiro[indoline-3,2'-thiazolidine]-4'-carboxylate (4e)

Overall yield 58%.$[\alpha]^{25}_D$ -5.7 (c 0.1, MeOH). ^{1}H NMR (400 MHz,$CDCl_3$) δ 1.38 (t, 3H, C*H*$_3$); 2.34 (s, 3H, C*H*$_3$); 3.34 (d, 1H, *J* = 11.6 Hz, H-5'a); 3.98 (dd, 1H, *J* = 6.0 and 11.6 Hz, H-5'b); 4.38 (q, 2H, C*H*$_2$); 4.85 (d, 1H, *J* = 6.0 Hz, H-4'); 6.72 (d, 1H, *J* = 8.0 Hz, H-7); 7.03 (d, 1H, H-6); 7.33 (d, 2H, *J* = 8.0 Hz, aryl); 7.44 (d, 2H, aryl); 7.54 (s, 1H, H-4); 8.06 (s, 1H, N*H*). ^{13}C NMR (100 MHz,$CDCl_3$) δ: 14.5 (*C*H$_3$), 21.5 (*C*H$_3$), 34.5 (C-5'), 62.7 (*C*H$_2$), 66.7 (C-4'), 72.5 (C-2'), 110.2, 126.1, 128.4, 129.0, 130.8, 133.6, 136.2, and 138.4 (aryl), 167.6, 170.1, and 176.2 (C=O). ESIMS m/z calcd for. per $C_{21}H_{19}ClN_2O_4S$, 430.08; found, 430.08.

(2'*S*,4'*R*)-ethyl 5-bromo-3'-(4-chlorobenzoyl)-2-oxospiro[indoline-3,2'-thiazolidine]-4'-carboxylate (4f)

Overall yield 46%. $[\alpha]^{25}_D$ -9.8 (c 0.24, MeOH). ^{1}H NMR (400 MHz,$CDCl_3$) δ 1.40 (t, 3H, C*H*$_3$); 3.35 (d, 1H, *J* = 12.0 Hz, H-5'a); 3.89 (dd, 1H, *J* = 6.0 and 11.8 Hz, H-5'b); 4.42 (q, 2H, C*H*$_2$); 4.84 (d, 1H, *J* = 6.0 Hz, H-4'); 7.36-7.50 (m, 5H, H-7, aryl); 7.78-7.81 (m, 2H, H-6, H-4); 8.04 (s, 1H, NH). ^{13}C NMR (100 MHz,$CDCl_3$) δ 14.5 (*C*H$_3$), 35.3 (C-5'), 63.1 (*C*H$_2$), 66.7 (C-4'), 72.3 (C-2'), 116.8, 118.8, 128.4, 128.6, 128.7, 129.2, 131.2, 139.3, and 140.9 (aryl), 168.7, 170.1, and 173.6 (C=O). ESIMS m/z calcd for. per $C_{20}H_{16}Br\ ClN_2O_4S$, 493.97; found, 494.09.

(2'*R*,4'*R*)-ethyl 5-bromo-3'-(4-chlorobenzoyl)-2-oxospiro[indoline-3,2'-thiazolidine]-4'-carboxylate (4g)

Overall yield 15%. $[\alpha]^{25}_{D}$ -6.9 (c 0.11, MeOH). ^{1}H NMR (400 MHz,$CDCl_3$) δ 1.24 (t, 3H, C*H*$_3$); 3.61-3.62 (m, 2H, H-5'a, H-5'b); 4.25 (q, 2H, C*H*$_2$); 5.43 (t, 1H, *J* = 9.6 Hz, H-4'); 7.45 (d, 2H, *J* = 8.4 Hz, aryl); 7.61 (d, 1H, *J* = 9.2 Hz, H-7); 7.79 (s, 1H, H-4); 8.05 (d, 2H, aryl); 8.90 (d, 1H, H-6); 9.51 (s, 1H, NH). ^{13}C NMR (100 MHz,$CDCl_3$) δ 14.4 (*C*H$_3$), 34.0 (C-5'), 62.4 (*C*H$_2$), 66.9 (C-2'), 78.8 (C-4'), 115.2, 122.2, 129.1, 129.6, 133.4, 134.7, 135.9, and 138.5 (aryl), 165.4, 170.0, and 172.5 (C=O). ESIMS m/z calcd for. per $C_{20}H_{16}BrClN_2O_4S$, 493.97; found, 494.09.

(2'*S*,4'*R*)-ethyl 3'-(4-chlorobenzoyl)-1-methyl-2-oxospiro[indoline-3,2'-thiazolidine]-4'-carboxylate (4h)

Overall yield 56%. $[\alpha]^{25}_{D}$ -8.9 (c 0.2, MeOH). ^{1}H NMR (400 MHz,$CDCl_3$) δ 1.36 (t, 3H, C*H*$_3$); 3.29 (s, 3H, C*H*$_3$); 3.38 (d, 1H, *J* = 11.6 Hz, H-5'a); 3.97 (dd, 1H, *J* = 6.0 and 11.6 Hz, H-5'b); 4.38 (q, 2H, C*H*$_2$); 4.85 (d, 1H, *J* = 5.6 Hz, H-4'); 6.84 (d, 1H, *J* = 8.0 Hz, H-7); 7.10 (t, 1H, *J* = 8.0 Hz, H-6); 7.31-7.38 (m, 3H, H-5, aryl); 7.41 (d, 2H, aryl); 7.76 (d, 1H, *J* = 7.6 Hz, H-4); 8.51 (s, 1H, NH). ^{13}C NMR (100 MHz,$CDCl_3$) δ 14.5 (*C*H$_3$), 26.1 (*C*H$_3$), 34.5 (C-5'), 62.8 (*C*H$_2$), 66.7 (C-4'), 72.5 (C-2'), 108.5, 123.4, 125.2, 128.4, 129.0, 130.4, 134.1, 137.3, and 141.4 (aryl), 168.1, 170.7, and 177.2 (C=O). ESIMS m/z calcd for $C_{21}H_{19}ClN_2O_4S$, 430.08; found, 430.08.

(2'*S*,4'*R*)-ethyl 3'-(4-chlorobenzoyl)-1,5-dimethyl-2-oxospiro[indoline-3,2'-thiazolidine]-4'-carboxylate (4i)

Overall yield 41%. $[\alpha]^{25}_{D}$ -15.2° (c 0.4, MeOH). ^{1}H NMR (400 MHz,$CDCl_3$) δ 1.37 (t, 3H, C*H*$_3$); 2.35 (s, 3H, C*H*$_3$); 3.33 (d, 1H, *J* = 12.0 Hz, H-5'a); 3.49 (s, 3H, C*H*$_3$); 4.00 (dd, 1H, *J* =

5.8 and 12.0 Hz, H-5'b); 4.38 (q, 2H, CH_2); 4.85 (d, 1H, J = 5.8 Hz, H-4'); 6.76 (d, 1H, J = 7.8 Hz, H-7); 7.12 (d, 1H, H-6); 7.33 (d, 2H, J = 7.6 Hz, aryl); 7.41 (d, 2H, aryl); 7.56 (s, 1H, H-4). ^{13}C NMR (100 MHz, $CDCl_3$) δ 14.5 (CH_3), 22.9 (CH_3), 29.8 (CH_3), 34.5 (C-5'), 62.8 (CH_2), 66.7 (C-4'), 72.5 (C-2'), 108.5, 123.4, 125.2, 128.4, 129.0, 130.4, 134.1, 137.3, and 141.4 (aryl), 168.1, 170.7, and 177.2 (C=O). ESIMS m/z calcd for $C_{22}H_{21}ClN_2O_4S$, 446.09; found, 446.11.

(2'*S*,4'*R*)-ethyl-5-bromo-3'-(4-chlorobenzoyl)-1-methyl-2-oxospiro[indoline-3,2'-thiazolidine]-4'-carboxylate (4j)

Overall yield 54%. $[\alpha]^{25}_D$ -21.2° (c 0.4, MeOH). ^{1}H NMR (400 MHz,$CDCl_3$) δ 1.48 (t, 3H, CH_3); 3.32 (d, 1H, J = 12.4 Hz, H-5'a); 3.48 (s, 1H, CH_3); 3.94-3.99 (m, 1H, H-5'b); 4.40 (q, 2H, CH_2); 4.87 (d, 1H, J = 6.2 Hz, H-4'); 7.38-7.47 (m, 4H, aryl); 7.52 (d, 1H, J = 8.0 Hz, H-6); 7.79-7.83 (m, 2H, aryl). ^{13}C NMR (100 MHz,$CDCl_3$) δ 14.7 (CH_3), 25.1 (CH_3), 35.3 (C-5'), 63.2 (CH_2), 66.7 (C-4'), 72.8 (C-2'), 116.9, 128.7, 128.9, 129.0, 129.1, 131.4, 133.5, 137.9, 139.1 (aryl), 168.5, 169.4, and 175.4 (C=O). ESIMS m/z calcd for $C_{21}H_{18}BrClN_2O_4S$, 507.99; found, 508.04.

(2'*S*,4'*R*)-ethyl-5-bromo-3'-(2-(4-chlorophenyl)acetyl)-1-methyl-2-oxospiro[indoline-3,2'-thiazolidine]-4'-carboxylate (4k)

Overall yield 38%. $[\alpha]^{25}_D$ -26.3° (c 0.11, MeOH). ^{1}H NMR (400 MHz,$CDCl_3$) δ 1.41 (t, 3H, CH_3); 3.20 (s, 3H, CH_3); 3.47 (d, 1H, J = 12.0 Hz, H-5'a); 3.63 (s, 2H, CH_2); 3.94 (dd, 1H, J = 6.0 and 11.6 Hz, H-5'b); 4.38 (q, 2H, CH_2); 5.06 (d, 1H, J = 6.0, H-4'); 6.66 (d, 1H, J = 8.4 Hz, H-7); 7.10 (d, 2H, J = 8.0 Hz, aryl); 7.27 (d, 2H, aryl); 7.39 (d, 1H, H-6); 7.60 (s, 1H, H-4). ^{13}C NMR (100 MHz,$CDCl_3$) δ 14.5 (CH_3), 27.0 (CH_3), 34.1 (C-5'), 41.7 (CH_2), 63.1 (CH_2), 64.5 (C-4'), 75.7 (C-2'), 110.1, 115.8, 127.8, 128.9, 129.2, 130.6, 132.9, 133.1, and 142.8 (aryl), 170.3, 174.3, and 177.8 (C=O). ESIMS m/z calcd for $C_{22}H_{20}BrClN_2O_4S$, 522.00; found 522.06.

(2'*S*,4'*R*)-ethyl 5-bromo-3'-benzoyl-1-methyl-2-oxospiro[indoline-3,2'-thiazolidine]-4'-carboxylate (4l)

Overall yield 32%. $[\alpha]^{25}_{D}$ -16.9° (c 0.5, MeOH). ^{1}H NMR (400 MHz,$CDCl_3$) δ 1.45 (t, 3H, C*H*$_3$); 3.29(s, 3H, C*H*$_3$); 3.36 (d, 1H, *J* = 12.4 Hz, H-5'a); 3.96-4.01 (m, 1H, H-5'b); 4.37 (q, 2H, C*H*$_2$); 4.91 (d, 1H, *J* = 6.2 Hz, H-4'); 6.73 (d, 1H, *J* = 8.0 Hz, H-7); 7.38-7.51 (m, 6H, H-6 and aryl); 7.91 (s, 1H, H-4). ^{13}C NMR (100 MHz,$CDCl_3$) δ 14.5 (*C*H$_3$), 25.6 (*C*H$_3$), 35.4 (C-5'), 63.1 (*C*H$_2$), 66.9 (C-4'), 73.1 (C-2'), 118.4, 127.5, 127.3, 128.2, 129.4, 133.5, 137.7, 139.2 (aryl), 168.8, 169.6, and 175.0 (C=O). ESIMS m/z calcd for $C_{20}H_{17}BrN_2O_4S$, 460.01; found, 460.09.

(2'*S*,4'*R*)-ethyl 5-bromo-1-methyl-3'-(4-methylbenzoyl)-2-oxospiro[indoline-3,2'-thiazolidine]-4'-carboxylate (4m)

Overall yield 37%. $[\alpha]^{25}_{D}$ -14.2° (c 0.3, MeOH). ^{1}H NMR (400 MHz,$CDCl_3$) δ 1.40 (t, 3H, C*H*$_3$); 2.35 (s, 3H, C*H*$_3$); 3.28 (s, 3H, C*H*$_3$); 3.32 (d, 1H, *J* = 11.6 Hz, H-5'a); 3.95 (dd, 1H, *J'* = 6.0 and 11.6 Hz H-5'b,); 4.39 (q, 2H, C*H*$_2$); 4.91 (d, 1H, *J* = 5.6 Hz, H-4'); 6.71 (d, 1H, *J* = 8.4 Hz, H-7); 7.14 (d, 2H, *J* = 7.6 Hz, aryl); 7.34 (d, 2H, aryl); 7.45 (d, 1H, H-6); 7.91 (s, 1H, H-4). ^{13}C NMR (100 MHz,$CDCl_3$) δ 14.5 (*C*H$_3$), 21.6 (*C*H$_3$), 27.0 (*C*H$_2$), 34.8 (C-5'), 62.8 (*C*H$_2$), 66.8 (C-4'), 72.5 (C-2'), 109.9, 115.9, 126.9, 128.3, 128.4, 129.4, 133.0, 141.3, and 143.0 (aryl), 169.4, 170.6, and 175.2 (C=O). ESIMS m/z calcd for $C_{22}H_{21}BrN_2O_4S$, 488.04; found, 488.11.

(2'*S*,4'*R*)-ethyl 5-bromo-3'-(cyclohexanecarbonyl)-1-methyl-2-oxospiro[indoline-3,2'-thiazolidine]-4'-carboxylate (4n)

Overall yield 49%. $[\alpha]^{25}_{D}$ – 37.3° (c 0.8, MeOH). (**A**) : ^{1}H NMR (400 MHz,$CDCl_3$) δ 1.15-1.22 (m, 4H, C*H*$_2$); 1.41 (t, 3H, C*H*$_3$); 1.64-1.78 (m, 6H, C*H*$_2$); 2.17 (t, 1H, C*H*); 3.20 (s, 3H, C*H*$_3$); 3.47 (d, 1H, *J* = 12.0 Hz, H-5'a); 3.97 (dd, 1H, *J'* = 6.0 and 11.6 Hz, H-5'b,); 4.41 (q, 2H, C*H*$_2$); 5.13 (d, 1H, *J* = 5.6 Hz, H-4'); 6.67 (d, 1H, *J* = 8.4 Hz, H-7); 7.39 (d, 1H, H-6); 7.57 (s,

1H, H-4). ^{13}C NMR (100 MHz,$CDCl_3$) δ 14.4 (*C*H_3), 25.8 (*C*H_2), 26.7 (*C*H_3), 30.2 (*C*H_2), 34.1 (C-5'), 44.1 (*C*H), 62.9 (*C*H_2), 64.1 (C-4'), 75.7 (C-2'), 110.0, 115.8, 127.6, 128.9, and 132.7 (aryl); 170.3, 174.3, and 177.8 (C=O); (**B**) : ^{1}H NMR (400 MHz,$CDCl_3$) δ 1.15-1.22 (m, 4H, C*H*$_2$); 1.41 (t, 3H, C*H*$_3$); 1.64-1.78 (m, 6H, C*H*$_2$); 2.17 (t, 1H, C*H*); 3.26 (s, 3H, C*H*$_3$); 3.34 (d, 1H, *J* = 12.0 Hz, H-5'a); 3.92 (dd, 1H, *J'* = 6.0 and 11.6 Hz, H-5'b,); 4.37 (q, 2H, C*H*$_2$); 5.52 (d, 1H, *J* = 5.2 Hz, H-4'); 6.77 (d, 1H, *J* = 8.4 Hz, H-7); 7.49 (d, 1H, H-6); 7.56 (s, 1H, H-4). ^{13}C NMR (100 MHz,$CDCl_3$) δ 14.4 (*C*H_3), 25.8 (*C*H_2), 26.9 (*C*H_3), 29.3 (*C*H_2), 33.9 (C-5'), 43.8 (*C*H), 62.2 (*C*H_2), 64.7 (C-4'), 75.7 (C-2'), 110.2, 115.9, 127.9, 129.0, and 132.7 (aryl); 170.1, 174.5, and 177.6 (C=O). ESIMS m/z calcd for $C_{21}H_{25}BrN_2O_4S$, 480.07; found, 480.15.

(2'S,4'R)-ethyl 5-methyl-3'-(cyclohexanecarbonyl)-1-methyl-2-oxospiro[indoline-3,2'-thiazolidine]-4'-carboxylate (4o)

Overall yield 47%. $[\alpha]^{25}_D$ -23.1° (c 0.5, MeOH). (**A**): ^{1}H NMR (400 MHz,$CDCl_3$) δ 1.15-1.26 (m, 4H, C*H*$_2$); 1.40 (t, 3H, C*H*$_3$); 1.63-1.73 (m, 6H, C*H*$_2$); 2.17 (t, 1H, C*H*); 2.30 (s, 3H, C*H*$_3$); 3.21 (s, 3H, C*H*$_3$); 3.45 (d, 1H, *J* = 12.0 Hz, H-5'a); 4.00 (dd, 1H, *J'* = 6.0 and 11.6 Hz, H-5'b,); 4.40 (q, 2H, C*H*$_2$); 5.13 (d, 1H, *J* = 5.6 Hz, H-4'); 6.67 (d, 1H, *J* = 8.0 Hz, H-7); 7.06 (d, 1H, H-6); 7.26 (s, 1H, H-4). ^{13}C NMR (100 MHz,$CDCl_3$) δ 14.5 (*C*H_3), 21.4 (*C*H_3), 25.7 (*C*H_2), 26.9 (*C*H_3), 29.2 (*C*H_2), 33.8 (C-5'), 44.2 (*C*H), 62.7 (*C*H_2), 64.2 (C-4'), 75.7 (C-2'), 108.3, 125.0, 126.5, 130.3, 132.7 and 143.0 (aryl); 170.5, 174.2, and 177.8 (C=O); (**B**): ^{1}H NMR (400 MHz,$CDCl_3$) δ 1.15-1.26 (m, 4H, C*H*$_2$); 1.40 (t, 3H, C*H*$_3$); 1.63-1.73 (m, 6H, C*H*$_2$); 2.17 (t, 1H, C*H*); 2.35 (s, 3H, C*H*$_3$); 3.25 (s, 3H, C*H*$_3$); 3.30 (d, 1H, *J* = 12.0 Hz, H-5'a); 3.94 (dd, 1H, *J'* = 6.0 and 11.6 Hz, H-5'b,); 4.36 (q, 2H, C*H*$_2$); 5.52 (d, 1H, *J* = 6.0 Hz, H-4'); 6.78 (d, 1H, *J* = 8.0 Hz, H-7); 7.18 (d, 1H, H-6); 7.64 (s, 1H, H-4). ^{13}C NMR (100 MHz,$CDCl_3$) δ 14.5 (*C*H_3), 21.1 (*C*H_3), 25.4 (*C*H_2), 25.8 (*C*H_3), 29.6 (*C*H_2), 32.2 (C-5'), 43.8 (*C*H), 62.0 (*C*H_2), 64.4 (C-4'), 75.8

(C-2'), 108.8, 126.4, 131.2, 132.9 and 143.2 (aryl); 170.7, 174.4, and 177.8 (C=O). ESIMS m/z calcd for $C_{22}H_{28}N_2O_4S$, 416.18; found, 416.24.

(2'*S*,4'*R*)- ethyl 3'-(cyclohexanecarbonyl)-1-methyl-2-oxospiro[indoline-3,2'-thiazolidine]-4'-carboxylate (4p)

Overall yield 45%. $[\alpha]^{25}_D$ -20.0° (c 0.4, MeOH). (**A**): ^{1}H NMR (400 MHz,$CDCl_3$) δ 1.13-1.24 (m, 4H, C*H*$_2$); 1.39 (t, 3H, C*H*$_3$); 1.62-1.79 (m, 6H, C*H*$_2$); 2.19 (t, 1H, C*H*); 3.23 (s, 3H, C*H*$_3$); 3.45 (d, 1H, *J* = 12.0 Hz, H-5'a); 3.99 (dd, 1H, *J'* = 6.0 and 11.6 Hz, H-5'b,); 4.38 (q, 2H, C*H*$_2$); 5.13 (d, 1H, *J* = 5.6 Hz, H-4'); 6.79 (d, 1H, *J* = 8.4 Hz, H-7); 7.02 (t, 1H, H-6); 7.27 (t, 1H, H-5); 7.46 (d, 1H, H-4). ^{13}C NMR (100 MHz,$CDCl_3$) δ 14.5 (*C*H$_3$), 25.7 (*C*H$_2$), 26.8 (*C*H$_3$), 29.2 (*C*H$_2$), 33.8 (C-5'), 44.1 (*C*H), 62.7 (*C*H$_2$), 64.2 (C-4'), 75.9 (C-2'), 108.5, 123.2, 124.2, 126.1, 129.9, 131.0, and 143.5 (aryl); 170.5, 174.2, and 177.8 (C=O); (**B**): ^{1}H NMR (400 MHz,$CDCl_3$) δ 1.13-1.24 (m, 4H, C*H*$_2$); 1.39 (t, 3H, C*H*$_3$); 1.62-1.79 (m, 6H, C*H*$_2$); 2.19 (t, 1H, C*H*); 3.28 (s, 3H, C*H*$_3$); 3.40 (d, 1H, *J* = 12.0 Hz, H-5'a); 3.95 (dd, 1H, *J'* = 6.0 and 11.6 Hz, H-5'b,); 4.31 (q, 2H, C*H*$_2$); 5.51 (d, 1H, *J* = 6.4 Hz, H-4'); 6.89 (d, 1H, *J* = 8.4 Hz, H-7); 7.14 (t, 1H, H-6); 7.38 (t, 1H, H-5); 7.46 (d, 1H, H-4). ^{13}C NMR (100 MHz,$CDCl_3$) δ 14.5 (*C*H$_3$), 25.7 (*C*H$_2$), 27.0 (*C*H$_3$), 29.3 (*C*H$_2$), 32.1 (C-5'), 42.9 (*C*H), 62.1 (*C*H$_2$), 65.3 (C-4'), 75.9 (C-2'), 109.0, 122.8, 125.1, 127.2, 128.2, 131.0, and 143.7 (aryl); 170.6, 174.0, and 177.6 (C=O). ESIMS m/z calcd for $C_{21}H_{26}N_2O_4S$, 402.16; found, 402.20.

(2'*S*,4'*R*)-ethyl 5-bromo-3'-(cyclohexanecarbonyl)-2-oxospiro[indoline-3,2'-thiazolidine]-4'-carboxylate (4q)

Overall yield 42%. $[\alpha]^{25}_D$ -27.1° (c 0.5, MeOH). ^{1}H NMR (400 MHz,$CDCl_3$) δ 1.15-1.22 (m, 4H, C*H*$_2$); 1.41 (t, 3H, C*H*$_3$); 1.64-1.78 (m, 6H, C*H*$_2$); 1.96 (t, 1H, C*H*); 3.43 (d, 1H, *J* = 12.0 Hz, H-5'a); 3.97 (dd, 1H, *J* = 6.0 and 11.6 Hz, H-5'b); 4.30 (q, 2H, C*H*$_2$); 4.63 (d, 1H, *J* = 6.0

Hz, H-4',); 7.49 (d, 1H, *J* = 8.4 Hz, H-7'); 7.68 (s, 1H, H-4'); 8.10 (d, 1H, H-6'). ^{13}C NMR (100 MHz,$CDCl_3$) δ 14.4 (*C*H_3), 25.8 (*C*H_2), 29.3 (*C*H_2), 39.0 (C-1), 44.9 (*C*H), 62.6 (*C*H_2), 65.0 (C-2), 75.7 (C-4), 118.8, 127.3, 128.0, 134.1, and 139.4 (aryl), 172.0, 175.9, and 177.4 (C=O). ESIMS m/z calcd for $C_{20}H_{23}BrN_2O_4S$, 466.06; found, 466.12.

(2'*SR*,4'*R*)-5-Bromo-3'-(cyclohexanecarbonyl)-1-methyl-2-oxospiro[indoline-3,2'-thiazolidine]-4'-carboxylic acid (4r)

Overall yield 37%. ^{1}H NMR (400 MHz,$CDCl_3$) (α) δ 1.14-1.38 (m, 6H, C*H*$_2$); 1.58-1.79 (m, 4H, C*H*$_2$); 2.27 (t, 1H, C*H*); 3.19 (s, 3H, C*H*$_3$); 3.54 (t, 1H, H-5'a); 3.88-3.91 (m, 1H, H-5'b); 5.11 (d, 1H, *J* = 6.8 Hz, H-4'); 6.64 (d, 1H, *J* = 8.0 Hz, H-7); 7.34 (d, 1H, H-6); 7.65 (s, 1H, H-4). **(β)** δ 1.14-1.38 (m, 6H, C*H*$_2$); 1.58-1.79 (m, 4H, C*H*$_2$); 2.27 (t, 1H, C*H*); 3.22 (s, 3H, C*H*$_3$); 3.54 (t, 1H, H-5'a); 3.81-3.85 (m, 1H, H-5'b); 5.37 (d, 1H, *J* = 5.6 Hz, H-4'); 6.74 (d, 1H, *J* = 8.0 Hz, H-7); 7.47 (d, 1H, H-6); 8.00 (s, 1H, H-4). ^{13}C NMR (100 MHz,$CDCl_3$) (α) δ 25.6 (*C*H_2), 26.3 (*C*H_2), 27.1 (*C*H_2), 29.4 (*C*H_2), 34.5 (C-5'), 43.3 (*C*H), 64.9 (C-4'), 71.4 (C-2'), 109.9, 115.6, 127.7, 129.2, 132.5 and 142.6 (aryl); 174.7, 175.3, and 176.9 (C=O). (β) δ 25.9 (*C*H_2), 26.9 (*C*H_2), 28.9 (*C*H_2), 29.9 (*C*H_2), 32.6 (C-5'), 43.7 (*C*H), 58.7 (C-4'), 69.8 (C-2'), 110.4, 116.7, 129.5, 129.9, 133.6 and 141.2 (aryl); 174.5, 175.2, and 176.7 (C=O). ESIMS m/z calcd for $C_{18}H_{19}BrN_2O_4S$, 438.02; found, 438.10.

General Procedure for the Synthesis of the (2'S, 4'R)-ethyl 1-Substituted-2-oxospiro[indoline-3,2'-thiazolidine]-4'-carboxylate Derivatives (5a-c). To a solution of indol-2,3-dione derivatives (**7-9**, 300 mg, 1.5 mmol) in dichloromethane was added 4-chlorobenzoyl chloride (1.8 mmol) and TEA (1.8 mmol). The reaction mixture was stirred at room temperature for 1 h and water was then added. The organic solution was washed with water (3x 100 mL), dried over Na_2SO_4, and evaporated in vacuo. Flash chromatography on silica gel, using ethyl

acetate/n-hexane as eluent, overall yielded the correspondent derivatives **19-21**. 1-substituted isatine **19-21** (150 mg, ~ 0,5 mmol) derivatives were dissolved in ethanol and cysteine ethyl ester and $NaHCO_3$ were added (0, 65 mmol). The mixture was stirred at room temperature for 12 h, then ethanol was filtrated and the surnatant was evaporated in vacuo. The crude was dissolved in dicholoromethane and washed with water (3 x 100 mL), the organic phase was dried over Na_2SO_4, and evaporated in vacuo. Flash chromatography on silica gel, using ethyl acetate/n-hexane as eluent, yielded the correspondent final derivatives **5a-c** as solid compounds.

(2'*S*,4'*R*)-ethyl 1-(4-chlorobenzoyl)-2-oxospiro[indoline-3,2'-thiazolidine]-4'-carboxylate (5a)

Overall yield 32%. $[\alpha]^{25}_{D}$+2.9° (c 0.4, MeOH). ^{1}H NMR (400 MHz,$CDCl_3$) δ 1.32 (t, 3H, C*H*$_3$); 3.34 (d, 2H, *J* = 5.6 Hz, H-5'); 4.27 (q, 2H, C*H*$_2$); 5.01 (dd, 1H, *J* = 5.5 and 13.0 Hz, H-4'); 7.08 (t, 1H, *J* = 7.6 Hz, H-6) 7.43 (d, 2H, *J* = 8.4 Hz, aryl); 7.59 (t, 1H, H-5); 7.81 (d, 1H, *J* = 7.6 Hz, H-7); 7.87 (d, 2H, aryl); 8.34 (d, 1H, *J* = 7.6 Hz, H-4). ^{13}C NMR (100 MHz,$CDCl_3$) δ 14.4 (*C*H$_3$), 40.8 (C-5'), 52.3 (C-4'), 62.8 (*C*H$_2$), 71.8 (C-2'), 120.9, 123.0, 129.1, 129.4, 131.7, 134.9, 137.5, 139.6, and 142.3 (aryl), 166.0, 172.1, and 190.6 (C=O). ESIMS m/z calcd for $C_{20}H_{17}ClN_2O_4S$, 416.06; found, 416.09.

(2'*S*,4'*R*)-ethyl 1-(4-chlorobenzoyl)-5-methyl-2-oxospiro[indoline-3,2'-thiazolidine]-4'-carboxylate (5b)

Overall yield 28%. $[\alpha]^{25}_{D}$ +3.21° (c 0.5, MeOH). ^{1}H NMR (400 MHz,$CDCl_3$) δ 1.31 (t, 3H, C*H*$_3$); 2.27 (s, 3H, C*H*$_3$); 3.34 (d, 2H, *J* = 5.2 Hz, H-5'); 4.28 (q, 2H, C*H*$_2$); 5.02 (d, 1H, *J* = 6.0 Hz, H-4'); 7.36-7.44 (m, 3H, H-7, aryl); 7.72 (m, 3H, H-6, aryl); 8.11 (s, 1H, H-4). ^{13}C NMR (100 MHz,$CDCl_3$) δ 14.3 (*C*H$_3$), 21.0 (*C*H$_3$), 40.7 (C-5'), 52.8 (C-4'), 62.5 (*C*H$_2$), 72.3 (C-2'),

120.8, 128.8, 128.9, 129.1, 129.3, 131.7, 132.0, 134.8, 138.4, and 140.5 (aryl), 166.2, 169.3, and 190.2 (C=O). ESIMS m/z calcd for $C_{21}H_{19}ClN_2O_4S$, 430.08; found, 430.15

(2'S,4'R)-ethyl 5-bromo-1-(4-chlorobenzoyl)-2-oxospiro[indoline-3,2'-thiazolidine]-4'-carboxylate (5c)

Overall yield 36%. $[\alpha]^{25}_D$ +2.2 (c 0.4, MeOH). ^{1}H NMR (400 MHz,$CDCl_3$) δ 1.31 (t, 3H, C*H*$_3$); 3.68 (d, 2H, *J* = 5.2 Hz, H-5'); 4.25 (q, 2H, C*H*$_2$); 5.03 (dd, 1H, *J* = 5.2 and 12.0 Hz, H-4'); 7.12 (d, 1H, *J* = 7.6 Hz, N*H*); 7.37-7.43 (m, 3H, H-7, H-6, H4); 7.72 (d, 2H, *J* = 8.0 Hz, aryl); 7.86 (m, 2H, aryl). ^{13}C NMR (100 MHz,$CDCl_3$) δ 14.3 (*C*H$_3$), 30.9 (C-5'), 53.3 (C-4'), 62.5 (*C*H$_2$), 72.3 (C-2'), 128.8, 128.9, 129.1, 129.3, 131.7, 132.0, 134.8, 138.4, and 140.7 (aryl), 166.3, 170.3, and 190.2 (C=O). ESIMS m/z calcd for $C_{20}H_{16}BrClN_2O_4S$, 493.97; found, 494.05.

(2'S,4'R)-ethyl 5-bromo-1-(cyclohexanecarbonyl)-2-oxospiro[indoline-3,2'-thiazolidine]-4'-carboxylate (5d)

Overall yield 25%.$[\alpha]^{25}_D$ -1.8 (c 0.1, MeOH). ^{1}H NMR (400 MHz,$CDCl_3$) δ 1.35 (t, 3H, C*H*$_3$); 1.39-1.48 (m, 4H, C*H*$_2$); 1.73-1.97 (m, 7H, C*H*$_2$ and C*H*); 3.23 (d, 1H, NH); 3.46 (dd, 1H, *J'* = 5.2, *J"* = 10.8 Hz, H-5'a); 3.93 (dd, 1H, *J'* = 7.6, *J"* = 10.8 Hz, H-5'b,); 4.31 (q, 2H, C*H*$_2$); 4.63 (t, 1H, H-4'); 7.49 (d, 1H, *J* = 8.8 Hz, H-7); 7.67 (s, 1H, H-4); 8.10 (d, 1H, H-6). ^{13}C NMR (100 MHz,$CDCl_3$) δ 14.4 (*C*H$_3$), 25.8 (*C*H$_2$), 26.0 (*C*H$_2$), 29.2 (*C*H$_2$), 39.1 (C-5'), 45.0 (*C*H), 62.5 (*C*H$_2$), 65.0 (C-4'), 75.8 (C-2'), 118.8, 127.3, 128.0, 134.1 and 139.4 (aryl); 172.0, 175.9 and 177.4 (C=O). ESIMS m/z calcd for $C_{20}H_{23}BrN_2O_5S$, 466.06; found, 466.10.

Ethyl 1-(4-chlorobenzoyl)-5-methyl-2-oxo-5'*H*-spiro[indoline-3,2'-thiazole]-4'-carboxylate (6b)

Overall yield 11%. ^{1}H NMR (400 MHz,$CDCl_3$) δ 1.36 (t, 3H, C*H*$_3$); 3.49 (s, 3H, C*H*$_3$); 4.39 (q, 2H, C*H*$_2$); 4.59 (dd, 2H, *J'* = 16.4 Hz, *J"* = 14.0 Hz, H-5); 7.26 (s, 1H, H-4); 7.32 (d, 1H, *J* =

8.0 Hz, H-7); 7.41-7.49 (m, 3H, aryl and H-6); 7.69 (d, 2H, *J* = 8.0 Hz, aryl). ^{13}C NMR (100 MHz,$CDCl_3$) δ 29.9 (*C*H_3), 45.5 (C-1), 53.8 (*C*H_3), 74.8 (C-2), 115.7, 126.3, 128.9, 130.3, 131.0, 131.6 and 155.4 (aryl), 172.7, 176.9, and 179.3 (C=O). ESIMS m/z calcd for $C_{21}H_{19}ClN_2O_4S$, 430.08; found, 430.12.

Ethyl 5-bromo-1-(4-chlorobenzoyl)-2-oxo-5'*H*-spiro[indoline-3,2'-thiazole]-4'-carboxylate (6c)

Overall yield 8%. ^{1}H NMR (400 MHz,$CDCl_3$) δ 1.35 (t, 3H, C*H*$_3$); 4.29-4.36 (m, 4H, C*H*$_2$ and H-5); 7.47-7.53 (m, 3H, aryl and H-7'); 7.63-7.70 (m, 3H, aryl and H-4'); 8.14 (d, 1H, *J* = 8.0 Hz, H-6'). ^{13}C NMR (100 MHz,$CDCl_3$) δ 14.8 (*C*H_3), 44.8 (C-1), 62.9 (*C*H_2), 74.1 (C-2), 115.7, 119.3, 125.8, 127.7, 128.4, 129.9, 133.5, 139.3 and 156.6 (aryl), 173.1, 175.9, and 178.2 (C=O). ESIMS m/z calcd for $C_{20}H_{14}BrClN_2O_4S$, 491.95; found, 492.03.

Ethyl 5-bromo-1-(cyclohexanecarbonyl)-2-oxo-5'*H*-spiro[indoline-3,2'-thiazole]-4'-carboxylate (6d)

Overall yield 12%. ^{1}H NMR (400 MHz,$CDCl_3$) δ 1.18-1.26 (m, 4H, C*H*$_2$); 1.39 (t, 3H, C*H*$_3$); 1.48-1.53 (m, 2H, C*H*$_2$); 1.62-1.70 (m, 4H, C*H*$_2$); 1.96 (t, 1H, C*H*); 4.42 (q, 2H, C*H*$_2$); 4.64 (dd, 2H, *J'* = 12.0 Hz, *J''* = 1Hz, H-5); 7.52 (d, 1H, *J* = 8.0 Hz, H-7'); 7.58 (s, 1H, H-4'); 8.12 (d, 1H, H-6'). ^{13}C NMR (100 MHz,$CDCl_3$) δ 14.8 (*C*H_3), 25.6 (*C*H_2), 30.1 (*C*H_2), 44.4 (C-1), 45.6 (*C*H), 62.8 (*C*H_2), 74.4 (C-2), 118.2, 127.9, 128.6, 133.7, 139.5 and 156.3 (aryl), 172.6, 176.9, and 178.3 (C=O). ESIMS m/z calcd for $C_{20}H_{21}BrN_2O_4S$, 464.04; found, 464.11.

Biology

Dulbecco's modified Eagle's medium (DMEM), fetal bovine serum (FBS), trypsin-EDTA solution (1x), penicillin and streptomycin, phosphate-buffered saline (PBS) were from Cambrex

Biosciences. 3-(4,5-Dimethylthiazol-2-yl)-2,5- diphenyltetrazolium bromide (MTT), propidium iodide (PI), Triton X-100, sodium citrate, formamide, were purchased from Sigma (Milan, Italy). Rabbit polyclonal anti-caspase-3, anti-MDM2, anti-Bcl-$x_{S/L}$, mouse monoclonal anti-actin, anti-p53, anti p21, anti p27, anti cytochrome C were purchased from Santa Cruz Biotechnology (DBA; Milan, Italy). ECL reagent was obtained from Amersham Pharmacia Biotech, U.K.

Cell Culture. Human prostate cancer (PC 3), human histiocytic lymphoma (U937), human lung adenocarcinoma (Calu), human hepatoma (HepG2), human anaplastic thyroid carcinoma (C643) human breast cancer (MCF-7) cell lines and human primary gingival fibroblasts were grown at 37 °C in Dulbecco's modified Eagle's medium containing 10 mM glucose (DMEMHG) supplemented with 10% fetal calf serum and 100 units/mL each of penicillin and streptomycin and 2 mmol/L glutamine. In each experiment, cells were placed in fresh medium, cultured in the presence of synthesized compounds (from 0.1 to 25 mM), and followed for further analyses.

Cell Viability Assay. Cell viability was determined using the 3-[4,5- dimethylthiazol-2,5-diphenyl-2H-tetrazolium bromide (MTT) colorimetric assay. The test is based on the ability of mitochondrial dehydrogenase to convert, in viable cells, the yellow MTT reagent (Sigma Chemical Co., St. Louis, MO) into a soluble blue formazan dye. Cells were seeded into 96-well plates to a density of 10^5 cells/100 μL well. After 24 hrs of growth to allow attachment to the wells, compounds were added at various concentrations (from 0.1 to 25 mM). After 24 or 48 h of growth and after removal of the culture medium, 100 μL/well of medium containing 1 mg/mL of MTT was added. Microplates were further incubated at 37 °C for 2 hrs in the dark. The solution was then gently aspirated from each well, and the formazan crystals within the cells were dissolved with 100 μL of DMSO. Optical densities were read at 550 nm using a Multiskan Spectrum Thermo Electron Corporation reader. Results were expressed as percentage relative to

vehicle-treated control (0.5% DMSO was added to untreated cells). IC_{50} (concentration eliciting 50% inhibition) values were determined by linear and polynomial regression. Experiments were performed in triplicate.

In vitro inhibition of p53-MDM2 interaction assay

We performed an in vitro binding assay using ImmunoSet™ p53/MDM2 complex ELISA set (Enzo Life Sciences). The assay was performed according to manufacturer's directions . Briefly, 96 multiwell was coated with p53 capture antibody and left over night at RT. Then, coating solution was removed and 200 microl of blocking buffer were added to each wells. The plate was incubated 1 hour at RT. Blocking buffer was then removed and 100 microl of p53/MDM2 standards were added to wells (except blank), in presence of 5 micromolar of indicated inhibitors. The plate was incubated 1 hour at RT on a plate shaker. Each wells were washed 4 times with 200 microl of wash buffer and 100 microl of MDM2 Detection antibody were added to wells (except blank) for 1 hour at RT. The plate was washed again and 100 microl of SA-HRP conjugated antibody were added to wells (except blank). The plate was incubated for 30 min at RT on a plate shaker. The wells were washed again and 100 microl of TMB (3,3',5,5' tetramethylbenzidine) were added to each well for 30 minutes at RT. To stop reaction 100 microl of 1N HCl were added to wells. After blanking the plate reader against the substrate, optical density was read at 450 nm. Data was presented as % of inhibition refer to Control (only standards).

Cell cycle analysis. Cells ($1x10^5$) were harvested when subconfluent, fixed in 70% ethanol for 1 h at -20°C, rehydrated in PBS, and the pellet was resuspended in 300µL PBS containing 250µg/ml RNAseA and 10µg/ml Propidium Iodide for 30 min in the dark. Samples were acquired with a CYAN flow cytometer (DAKO Corporation, San Jose, CA, USA). The cell cycle

distribution, expressed as percentage of cells in the G0/G1, S, and G2/M phages, was calculated using SUMMIT software

Annexin V assay. Cells were plated at $1x10^5$ in six-well plates and washed with PBS1X and then with Annexin V Binding Buffer. After centrifugation at 2000 rpm for 5 min, the cells were resuspended in 100ul of Annexin V Binding Buffer and incubated with 5 μl of FITC Annexin V (BioLegend) and 2 μl of 500 μg/ml Propidium Iodide for 15 min at 25°C in the dark. Finally, 400 μl of Annexin V Binding Buffer were added to each test tube. Samples were acquired with a CYAN flow cytometer (DAKO Corporation, San Jose, CA, USA) and analysed using SUMMIT software.

Western Blotting and Immunoprecipitation Analysis. MCF-7 cells were plated in Petri dishes (1x106 cells) in normal culture conditions and incubated with or without **4n** and Nutlin.At the indicated times, cells were lysed using an ice cold lysis buffer (50 mM Tris, 150 mM NaCl, 10 mM EDTA, 1% Triton) supplemented with a mixture of protease inhibitors containing antipain, bestatin, chymostatin, leupeptin, pepstatin, phosphoramidon, Pefabloc, EDTA, and aprotinin (Boehringer, Mannheim, Germany). Equivalent amounts of protein were loaded on 8-12% sodium dodecyl sulfate (SDS)- polyacrylamide gels and electrophoresed followed by blotting onto nitrocellulose membranes (Bio-Rad, Germany). After blotting with 5% (w/v) fat-free milk powder and 0.1% Tween 20 in TBS, the membrane was incubated overnight at 4 °C with specific antibodies at the concentrations indicated by the manufacter's protocol (Santa Cruz Biotechnology). The antibody was diluted in Tris-buffered saline/Tween 20 5% milk powder. Following incubation with horseradish peroxidase-conjugated secondary antibodies, bands were detected by enhanced chemiluminescence (ECL kit, Amersham, Germany). Each filter was then probed with mouse monoclonal anti-actin antibody. Level of expression of detected bands was

quantified by NIH ImageJ 1.40 after normalization with β-actin. For immunoprecipitation, cells were lysed in immunoprecipitation buffer (0.05 mol/l Tris–HCl (pH 8.0),0.005 mol/l EDTA, 0.15 mol/l NaCl, 1% Nonidet P-40, 0.5% sodium deoxycolate, 0.1% SDS, 0.01 mol/l NaF, 0.005 mol/l EGTA, 0.01 mol/l sodium pyrophosphate, and 0.001 mol/l phenylmethylsulfonylfluoride). Rabbit polyclonal antibody reactive to MDM2 (Santa Cruz Biotechnology, Santa Cruz, CA, USA) and protein G plus/protein A agarose beads (Oncogene Science, Boston, MA, USA) were used to immunoprecipitate MDM2 from 1 mg total lysate. Mouse monoclonal antibodies to total p53 were from Santa Cruz Biotechnology.

Molecular Modeling Methods.

The new version of the docking program AutoDock**Error! Bookmark not defined.** as implemented through the graphical user interface called AutoDockTools (ADT), was used to dock into the MDM2 structure **4n** and the co-crystal ligand. The MDM2 structure was retrieved from the Protein Data Bank (PDB code 1LBL)[28] and co-crystal waters and ligand removed. **4n** was built using the builder in the Maestro package of Schroedinger Suite 2007 and optimized using a version of MacroModel also included. The constructed compounds and the receptor structure were converted to AD4 format files using ADT generating automatically all other atom values. The docking area was centered around the putative binding site. A set of grids of 60 Å × 60 Å × 60 Å with 0.375 Å spacing was calculated around the docking area for the ligand atom types using AutoGrid4. For each ligand, 100 separate docking calculations were performed. Each docking calculation consisted of 10 million energy evaluations using the Lamarckian genetic algorithm local search (GALS) method. The GALS method evaluates a population of possible docking solutions and propagates the most successful individuals from each generation into the

subsequent generation of possible solutions. A low-frequency local search according to the method of Solis and Wets is applied to docking trials to ensure that the final solution represents a local minimum. All dockings described in this paper were performed with a population size of 250, and 300 rounds of Solis and Wets local search were applied with a probability of 0.06. A mutation rate of 0.02 and a crossover rate of 0.8 were used to generate new docking trials for subsequent generations, and the best individual from each generation was propagated over the next generation. The docking results from each of the 100 calculations were clustered on the basis of root-mean square deviation (rmsd) (solutions differing by less than 2.0 Å) between the Cartesian coordinates of the atoms and were ranked on the basis of free energy of binding (ΔG_{AD4}). Because AD4 does not perform any structural optimization and energy minimization of the complexes found, a molecular mechanics/energy minimization (MM/EM) approach was applied to refine the AD4 output. The computational protocol applied consisted of the application of 100000 steps of the Polak−Ribiére conjugate gradients (PRCG) or until the derivative convergence was 0.05 kJ/mol. **4n**/MDM2 complex picture was rendered employing the UCSF Chimera software.[38]

ASSOCIATED CONTENT

Supporting Information. Microanalytical data for all test compounds. ^{1}H, ^{13}C and ROESY spectra of compound **4n**. In vitro p53/MDM2 binding assay results. This material is available free of charge via the Internet at http://pubs.acs.org."

AUTHOR INFORMATION

Corresponding Author

*. E-mail: imgomez@unina.it or

E-mail: pcampiglia@unisa.it

Author Contributions

The manuscript was written through contributions of all authors. All authors have given approval to the final version of the manuscript.

ACKNOWLEDGMENT

The ESIMS and NMR spectral data were provided by Centro di Ricerca Interdipartimentale di Analisi Strumentale, Università degli Studi di Napoli "Federico II". The assistance of the staff is gratefully appreciated. This work was supported by grants from Italian Ministero dell'Istruzione, Università e Ricerca (PRIN 20098SJX4F-002)

ABBREVIATIONS

MDM2, mouse double minute 2 homolog; EtOH, ethanol; THF, tetrahydrofuran; TEA, triethylamine; NOE, nuclear Overhauser effect; DCM, dichloromethane; $NaHCO_3$, sodium bicarbonate; SD, standard deviation; FACS, fuorescence activated cell sorting; SEM, standard error of the mean; TLC, thin-layer chromatography; MS, mass spectrometry; ESI, electrospray

ionization; DMSO, dimethylsulfoxide; PBS, phosphate buffered saline; EDTA, ethylenediaminetetraacetic acid; TBS, Tris buffered saline.

REFERENCES

(1) Levine, J.; Oren M. The first 30 years of p53: Growing ever more complex. *Nat. Rev. Cancer* **2009,** *9*, 749–758.

(2) Vogelstein, B.; Lane, D.; Levine, A. J. Surfing the p53 network. *Nature* **2000**, *408*, 307–310.

(3) Vousden, K. H.; Prives, C. Blinded by the light: The growing complexity of p53. Cell **2009**, *137*, 413–431.

(4) Feng, Z.; Wu, R.; Lin, M.; Hu, W. Tumor suppressor p53: new functions of an old protein *Front. Biol.* **2011**, *6*, 58–68

(5) Maddocks, O. D. K.; Vousden, K. H. Metabolic regulation by p53 *J. Mol. Med.* **2011**, *89*, 237–245

(6) Muller, P. A. J.; Vousden, K. H.; Norman, J. C. p53 and its mutants in tumor cell migration and invasion *J. Cell Biol*. **2011**, *192*, 209–218 and references therein

(7) Yang, Y.; Li, C. C. Weissman, A. M. Regulating the p53 system through ubiquitination. *Oncogene* **2004**, *23*, 2096–2106.

(8) Momand, J.; Zambetti, G. P.; Olson, D. C.; George, D.; Levine, A. The mdm-2 oncogene product forms a complex with p53 protein and inhibits p53-mediated transactivation. *Cell* **1992**, *69*, 1237–1245.

(9) Geyer RK, Yu ZK, Maki CG. The MDM2 RING-finger domain is required to promote p53 nuclear export. *Nat Cell Biol.* **2000**, *2*, 569–73.

(10) Haupt, Y.; Maya, R.; Kazaz, A.; Oren, M. Mdm2 promotes the rapid degradation of p53. *Nature* **1997**, *387*, 296–299.

(11) a) Levine, A. p53, the cellular gatekeeper for growth and division. *Cell* **1997**, *88*, 323-331. b) Greenblatt, M. S.; Bennett, W. P.; Hollstein, M.; Harris, C.C. Mutations in the p53 tumor suppressor gene: clues to cancer etiology and molecular pathogenesis. *Cancer Res.* **1994**, *54*, 4855–4878.

(12) a) Fakharzadeh, S. S.; Trusko, S. P.; George, D. L. Tumorigenic potential associated with enhanced expression of a gene that is amplified in a mouse tumor cell line. *EMBO J.*, **1991**, *10*, 1565–1569. b) Oliner, J. D.; Kinzler, K. W.; Meltzer, P. S.; George, D. L.; Vogelstein, B. Amplification of a gene encoding a p53-associated protein in human sarcomas. *Nature* **1992**, *358*, 80–83. c) Jones, S. N.; Hancock, A. R.; Vogel, H.; Donehower, L. A.; Bradley, A. Overexpression of Mdm2 in mice reveals a p53-independent role for Mdm2 in tumorigenesis. *Proc. Natl. Acad. Sci. USA*, **1998**, *95*, 15608–15612.

(13) a) Ventura, A.; Kirsch, D. G.; McLaughlin, M. E.; Tuveson, D. A.; Grimm, J.; Lintault, L.; Newman, J.; Reczek, E. E.; Weissleder, R.; Jacks, T. Restoration of p53 function leads to tumor regression in vivo. *Nature* **2007**, *445*, 661−665. b) Xue, W.; Zender, L.; Miething, C.; Dickins, R. A.; Hernando, E.; Krizhanovsky, V.; Cordon-Cardo, C.; Lowe, S. W. Senescence and tumour clearance is triggered by p53 restoration in murine liver carcinomas. *Nature* **2007**, *445*, 656−660.

(14) a) Brown, C. J.; Lain, S.; Verma, C. S.; Fersht, A. R.; Lane, D. P. Awakening guardian angels: drugging the p53 pathway *Nature Rev. Cancer* **2009**, *9* , 862–873; b) Chene, P. Inhibiting the p53-MDM2 interaction: An important target for cancer therapy. *Nat. Rev. Cancer* **2003**, *3*, 102–109. (b) Hardcastle, I. R. Inhibitors of the MDM2-p53 interaction as anticancer drugs. *Drugs Fut.* **2007**, *32*, 883-896.

(15) a) Fischer, P. Peptide, peptidomimetic, and small-molecule antagonists of the p53-HDM2 protein-protein interaction. *Int. J. Pept. Res. Ther*. **2006**, *12*, 3–19. b) Shangary, S.; Wang, S. Small-molecule inhibitors of the MDM2-p53 protein-protein interaction to reactivate p53 function: A novel approach for cancer therapy. *Ann. Rev. Pharmacol. Toxicol*. **2009**, *49*, 223–241.

(16) Vassilev, L. T.; Vu, B. T.; Graves, B.; Carvajal, D.; Podlaski, F.; Filipovic, Z.; Kong, N.; Kammlott, U.; Lukacs, C.; Klein, C.; Fotouhi, N.; Liu, E. A. In vivo activation of the p53 pathway by small-molecule antagonists of MDM2. *Science* **2004**, *303*, 844–848.

(17) a) Grasberger, B. L.; Lu, T. B.; Schubert, C.; Parks, D. J.; Carver, T. E.; Koblish, H. K.; Cummings, M. D.; LaFrance, L. V.; Milkiewicz, K. L.; Calvo, R. R.; Maguire, D.; Lattanze, J.; Franks, C. F.; Zhao, S. Y.; Ramachandren, K.; Bylebyl, G. R.; Zhang, M.; Manthey, C. L.; Petrella, E. C.; Pantoliano, M. W.; Deckman, I. C.; Spurlino, J. C.; Maroney, A. C.; Tomczuk, B. E.; Molloy, C. J.; Bone, R. F. Discovery and cocrystal structure of benzodiazepinedione HDM2 antagonists that activate p53 in cells. *J. Med. Chem*. **2005**, *48*, 909–912. b) Koblish, H. K.; Zhao, S. Y.; Franks, C. F.; Donatelli, R. R.; Tominovich, R. M.; LaFrance, L. V.; Leonard, K. A.; Gushue, J. M.; Parks, D. J.; Calvo, R. R.; Milkiewicz, K. L.; Marugan, J. J.; Raboisson, P.; Cummings, M. D.; Grasberger,

B. L.; Johnson, D. L.; Lu, T. B.; Molloy, C. J.; Maroney, A. C. Benzodiazepinedione inhibitors of the Hdm2: p53 complex suppress human tumor cell proliferation in vitro and sensitize tumors to doxorubicin in vivo. *Mol. Cancer Ther*. **2006**, *5*, 160–169.

(18) a) Ding, K.; Lu, Y.; Nikolovska-Coleska, Z.; Qui, S.; Ding, Y.; Gao, W.; Stuckey, J.; Krajewski, K.; Roller, P. P.; Tomita, Y.; Parrish, D. A.; Deschamps, J. R.; Wang, S. Structure-based design of potent non-peptide MDM2 inhibitors. *J. Am. Chem. Soc.* **2005**, *127*, 10130–10131. c) Yu, S.; Qin, D.; Shangary, S.; Chen, J.; Wang, G.; Ding, K.; McEachern, D.; Qiu, S.; Nikolovska-Coleska, Z.; Miller, R.; Kang, S.; Yang, D.; Wang, S. Potent and Orally Active Small-Molecule Inhibitors of the MDM2-p53 Interaction. *J. Med. Chem*. **2009**, *52*, 7970–7973.

(19) Allen, J. G.; Bourbeau, M. P.; Wohlhieter, G. E.; Bartberger, M. D.; Michelsen, K.; Hungate, R.; Gadwood, R. C.; Gaston, R. D.; Evans, B.; Mann, L. W.; Matison, M. E.; Schneider, S.; Huang, X.; Yu, D.; Andrews, P. S.; Reichelt, A.; Long, A. M.; Yakowec, P.; Yang, E. Y.; Lee, T. A.; Oliner, J. D. Discovery and optimization of chromenotriazolopyrimidines as potent inhibitors of the mouse double minute 2-tumor protein 53 protein-protein interaction. *J. Med. Chem*. **2009**, *52*, 7044– 7053.

(20) a) Hardcastle, I. R.; Ahmed, S. U.; Atkins, H.; Farnie, G.; Golding, B. T.; Griffin, R. J.; Guyenne, S.; Hutton, C.; Kallblad, P.; Kemp, S. J.; Kitching, M. S.; Newell, D. R.; Norbedo, S.; Northen, J. S.; Reid, R. J.; Saravanan, K.; Willems, H. M. G.; Lunec, J. Small-molecule inhibitors of the MDM2-p53 protein-protein interaction based on an isoindolinone scaffold. *J. Med. Chem.* **2006**, *49*, 6209–6221. b) Hardcastle, I. R.; Junfeng Liu, J.; Valeur, E.; Watson, A.; Ahmed, S. U.; Blackburn, T. J.; Bennaceur, K.; Clegg,

W.; Drummond, C.;. Endicott, J. A.; Golding, B. T.; Griffin, R. J.; Gruber, J.; Haggerty, K.; Harrington, R. W.; Hutton, C., Kemp, S.; Lu, X.; McDonnell, J. M.; Newell, D. R.; Noble, M. E. M.; Payne,S. L.; Revill, C. H.; Riedinger, C.; Xu, Q.; Lunec, J. Isoindolinone inhibitors of the Murine Double Minute 2 (MDM2)-p53 protein-protein interaction: Structure-activity studies leading to improved potency. *J. Med. Chem*. **2011**, *54*, 1233–1243.

(21) a) Kussie, P. H.; Gorina, S.; Marechal, V.; Elenbaas, B.; Moreau, J.; Levine, A. J.; Pavletich, N. P. Structure of the MDM2 oncoprotein bound to the p53 tumor suppressor transactivation domain. *Science* **1996**, *274*, 948–953. b) Lee, H.; Mok, K. H.; Muhandiram, R.; Park, K. H.; Suk, J. E.; Kim, D. H.; Chang, J.; Sung, Y. C.; Choi, K. Y.; Han, K. H. Local structural elements in the mostly unstructured transcriptional activation domain of human p53. *J. Biol. Chem.* **2000**, *275*, 29426–29432.

(22) a) Murray, J. K.; Gellman, S. H. Targeting protein-protein interactions: lessons from p53/MDM2. *Biopolymers* **2007**, *88*, 657–686. b) Shangary, S.; Wang, S. Small-molecule inhibitors of the MDM2-p53 protein-protein interaction to reactivate p53 function: a novel approach for cancer therapy. *Annu. Rev. Pharmacol. Toxicol*. **2009**, *49*, 223–241.

(23) Gomez-Monterrey, I.; Bertamino, A.; Porta, A.; Carotenuto, A.; Musella, S.; Aquino, C.; Granata, I.; Sala, M.; Brancaccio, D.; Picone, D.; Ercole, C.; Stiuso, P.; Campiglia, P.; Grieco, P.; Ianelli, P.; Maresca, B.; Novellino, E. Identification of the Spiro(oxindole-3,3'-thiazolidine)-based derivatives as potential p53 activity modulators. *J. Med. Chem*. **2010**, *53*, 8319–8329.

(24) Bertamino, A.; Aquino, C.; Sala, M.; de Simone, N.; Mattia, C. A.; Erra, L.; Musella, S.; Iannelli, P.; Carotenuto, A.; Grieco, P.; Novellino, E.; Campiglia, P.; Gomez- Monterrey, I. Design and synthesis of spirotryprostatin-inspired diketopiperazine systems from prolyl spirooxoindolethiazolidine derivatives. *Bioorg. Med. Chem.* **2010**, *18*, 4328–4337.

(25) (a) Szilagyi, L.; Gyorgydeak, Z. Comments on the putative stereoselectivity in cysteine-aldehyde reactions. Selective C(2) inversion and C(4) epimerization in thiazolidine-4-carboxylic acids. *J. Am. Chem. Soc,* **1979**, *101*, 427-432. (b) Deroose F. D; De Clercq. J. Novel Enantioselective Syntheses of (+)-Biotin *J. Org. Chem.* **1995**, 60, 321-330.

(26) Neuhaus, D.; Williamson, M. P. The nuclear Overhauser effect in structural and conformational analysis. *Wiley-VCH,* **2000**, New York.

(27) (a) Arva, N. C.; Talbott, K. E.; Okoro, D. R.; Brekman, A.; Qiu, W. G.; Bargonetti, J. Disruption of the p53-Mdm2 complex by Nutlin-3 reveals different cancer cell phenotypes. *Ethn Dis.* **2008**, *18*, *S2*, 1-8. (b) Supiot, S.; Hill, R. P.; Bristow, R. G. Nutlin-3 radiosensitizes hypoxic prostate cancer cells independent of p53. *Mol Cancer Ther* **2008**,7, 993-999. (c) Zheng T.; Jiabei Wang J.; Song X.; Meng, X.; Pan, S.; Jiang, H.; Liu, L. Nutlin-3 cooperates with doxorubicin to induce apoptosis of human hepatocellular carcinoma cells through p53 or p73 signaling pathways. *J. Cancer Res. Clin. Oncol.* **2010**, *136*,1597–1604.

(28) Popowicz, G.M.; Czarna, A.; Wolf, S.; Wang, K.; Wang, W.; Dömling, A.; Holak, T.A. Structures of low molecular weight inhibitors bound to MDMX and MDM2 reveal new approaches for p53-MDMX/MDM2 antagonist drug discovery. *Cell Cycle* **2010**, *9*, 1104−1111.

(29) (a) Huey, R.; Morris, G. M.; Olson, A. J.; Goodsell, D. S. A semiempirical free energy force field with charge-based desolvation. *J. Comput. Chem*. **2007**, *28*, 1145−1152. (b) Cosconati, S.; Forli, S.; Perryman, A. L.; Harris, R.; Goodsell, D. S.; Olson, A. J. Virtual Screening with AutoDock: Theory and Practice. *Expert Opin. Drug Discovery* **2010**, *5*, 597−607.

(30) Gonzalez-Lopez de Turiso, F.; Sun, D.; Rew, Y.; Bartberger, M. D.; Beck, H. P.; Canon, J.; Chen, A.; Chow, D.; Correll, T. L.; Huang, X.; Julian, L. D.; Kayser, F.; Lo, M. C.; Long, A. M.; McMinn, D.; Oliner, J. D.; Osgood, T.; Powers, J. P.; Saiki, A. Y.; Schneider, S.; Shaffer, P.; Xiao, S. H.; Yakowec, P.; Yan, X.; Ye, Q.; Yu, D.; Zhao, X.; Zhou, J.; Medina, J. C.; Olson; S. H. Rational Design and Binding Mode Duality of MDM2–p53 Inhibitors. *J. Med. Chem.* 2013, *in press.*

(31) Vousden, K. H.; Xin Lu, X. Live or let die: the cell's response to p53. *Nat. Rev. Cancer,* **2002**, *2*, 594–604.

(32) Haupt, S.; Berger, M.; Goldberg, Z.; Haupt, Y. Apoptosis – the p53 network. *J. Cell Science* **2003**, *116*, 4077–4085

(33) Pietsch, E. C.; Sykes, S. M.; McMahon, S. B.; Murphy M. E. The p53 family and programmed cell death. *Oncogene.* **2008**, *27*, 6507–6521.

(34) Hori, T.; T Kondo, T.; Kanamori, M.; Tabuchi Y.; Ogawa, R.; Zhao, Q-L.; Ahmed, K.; Yasuda, T.; Seki, S.; Suzuki, K.; Kimura, T. Nutlin-3 enhances tumor necrosis factor-related apoptosis-inducing ligand (TRAIL)-induced apoptosis through up-regulation of death receptor 5 (DR5) in human sarcoma HOS cells and human colon cancer HCT116 cells. *Cancer Lett.* **2010,** *287*, 98–108.

(35) Tseng, H-Y.; Jiang, C. C.; Croft, A.; Tay, K. H.; Thorne, R. F.; Fan Yang, F.; Liu, H.; Hersey, P.; Zhang X. D. Contrasting Effects of Nutlin-3 on TRAIL- and Docetaxel-Induced Apoptosis Due to Upregulation of TRAIL-R2 and Mcl-1 in Human Melanoma Cells. *Mol Cancer Ther* **2010**, *9*, 3363-3374.

(36) Bax, A.; Davis, D. G. 2D ROESY with cw spinlock for mixing phase sensitive using States-TPPI method. *J. Magn. Reson.* **1985**, *63*, 207–213.

(37) States, D. J.; Haberkorn, R. A.; Ruben, D. J. A Two-dimensional nuclear Overhauser experiment with pure absorption phase four quadrants. *J. Magn. Reson.* **1982**, *48*, 286–292.

(38) Pettersen, E. F.; Goddard, T. D.; Huang, C. C.; Couch, G. S.; Greenblatt, D. M.; Meng, E. C.; Ferrin, T. E. UCSF Chimera - A visualization system for exploratory research and analysis. *J. Comput. Chem*. **2004**, *25*, 1605-1612

"Table of Contents Graphic"

Synthesis, in vitro, and in cell studies of a new series of [indoline-3,2'-thiazolidine]-based p53 modulators.

Alessia Bertamino, Maria Soprano, Simona Musella, Maria Rosaria Rusciano, Marina Sala,a Ermelinda Vernieri, Veronica Di Sarno, Antonio Limatola, Alfonso Carotenuto, Sandro Cosconati, Paolo Grieco, Ettore Novellino, Maddalena Illario, Pietro Campiglia, Isabel Gomez-Monterrey.